Federal Technology Alert
A New Technology Demonstration Publication
DOE/EE-0316
Federal Energy Management Program

Leading by example, saving energy and taxpayer dollars in federal facilities

Summary of Results from Testing a 30-kW-Microturbine and Combined Heat and Power (CHP) System

Frank E. Pierce, Jr.
Oak Ridge National Laboratory Integrated Energy System (IES) Test Laboratory

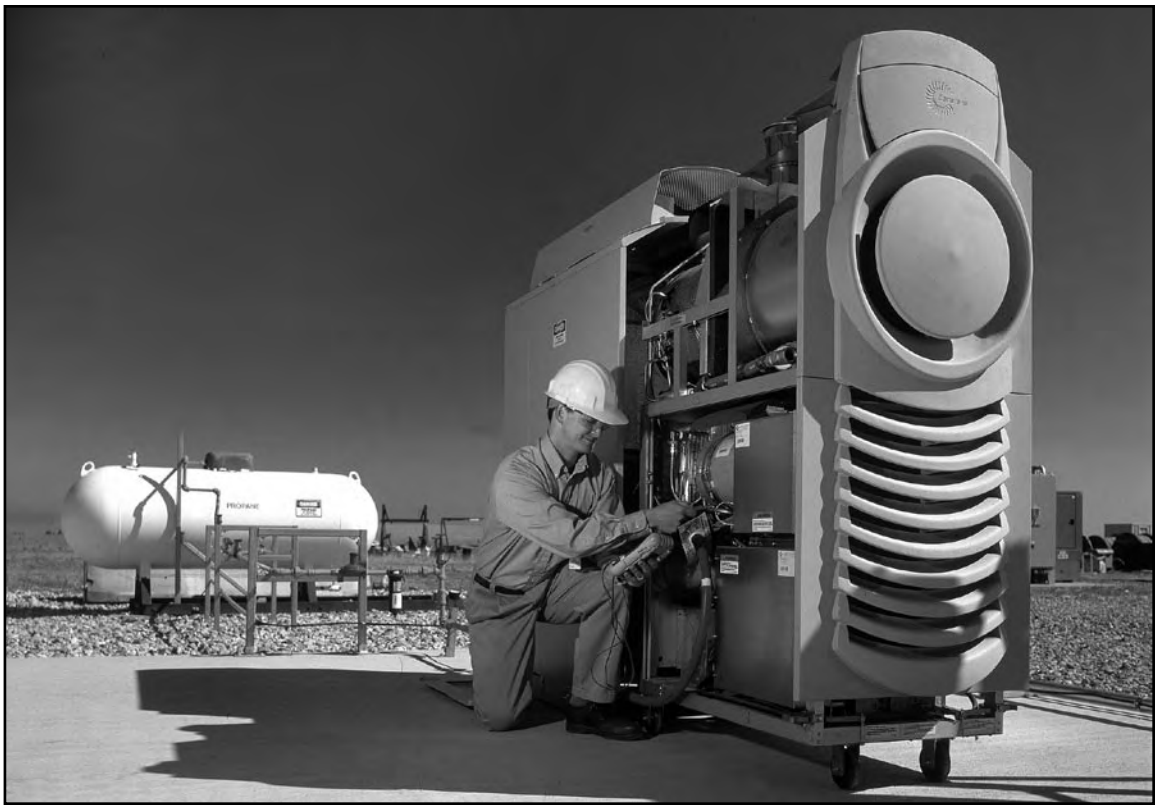

Abstract

A combined heat and power (CHP) system consists of a power generation system integrated with waste heat recovery configurations that can provide input for various thermally activated technologies (TATs). This publication summarizes in one document the results of a series of CHP system tests performed at the ORNL CHP Integration Test Facility. This document provides an energy manager who is considering installation of a microturbine-based CHP system a single source for performance, efficiency, and emissions test results for an individual microturbine or one integrated with TATs. The tests were performed using a 30-kW microturbine and TATs including an indirect-fired, single-effect absorption chiller, direct- and indirect-fired desiccant dehumidifiers, and an air-to-water heat exchanger.

Bringing you a prosperous future where energy is clean, abundant, reliable, and affordable

U.S. Department of Energy
Energy Efficiency and Renewable Energy

Internet: www.eere.energy.gov/femp/

LIST OF FIGURES

LIST OF TABLES

ACRONYMS

ABSC	absorption chiller	IES	integrated energy system
CHP	combined heat and power	IFDD	indirect-fired desiccant dehumidifiers
DER	distributed energy resource	LC	latent capacity
DFDD	direct-fired desiccant dehumidifiers	LCOP	latent coefficient of performance
DG	distributed generation	LiBr/water	lithium-bromide/water
HHV	higher heating value	MTG	microturbine generator
HRU	heat recovery unit	ORNL	Oak Ridge National Laboratory
HVAC	heating, ventilating, and air-conditioning	TAT	thermally activated technologies

Contents

1. ABOUT THE TECHNOLOGY

The U.S. Department of Energy's Office of Electricity Delivery and Energy Reliability studies the integration of electric power generation and thermally activated heating, ventilating, and air-conditioning (HVAC) systems. This program has sponsored research on a natural-gas-fired, microturbine-based combined heat and power (CHP) system with thermally activated technologies (TAT) at Oak Ridge National Laboratory's (ORNL's) CHP Integration Test Facility in Oak Ridge, Tennessee. This report summarizes the results of performance and efficiency tests on a microturbine distributed energy resource (DER). The microturbine was operated individually as well as integrated with various waste heat recovery configurations over a range of design and off-design conditions in steady-state operating mode. More detailed descriptions of the tests and results can be found in the references cited throughout this summary report.

DERs are small, modular, power-generation systems such as gas turbines, microturbines, fuel cells, and advanced reciprocating engines that are located in the vicinity of the energy end user. The major benefits of a DER are (1) local control of power generation, (2) efficient use of waste heat, (3) increased overall efficiency, and (4) a reduction in emissions.[1,2]

In a CHP system, waste heat from the DER generation system, which is normally discharged to the environment, is used as input power for TATs. Overall efficiencies of 40 to 70% or more can be achieved in well-integrated CHP systems when the waste heat is used. Technologies that can be driven by DER system waste heat include (1) chillers and desiccant dehumidifiers for space cooling and dehumidification, (2) steam generators for space heating, and (3) heat exchangers for process and domestic hot water.[1] These CHP systems can maximize energy efficiency, provide an option to central power generation, and improve electric power reliability and quality.[1,2]

2. ORNL CHP INTEGRATION TEST FACILITY

2.1 TEST FACILITY CONFIGURATION

The current CHP test facility configuration (Fig. 1) is flexible and contains a 30-kW natural-gas-fired microturbine, which can be integrated with various thermally activated HVAC systems. TATs currently in the CHP Integration Test Facility are a first-generation heat

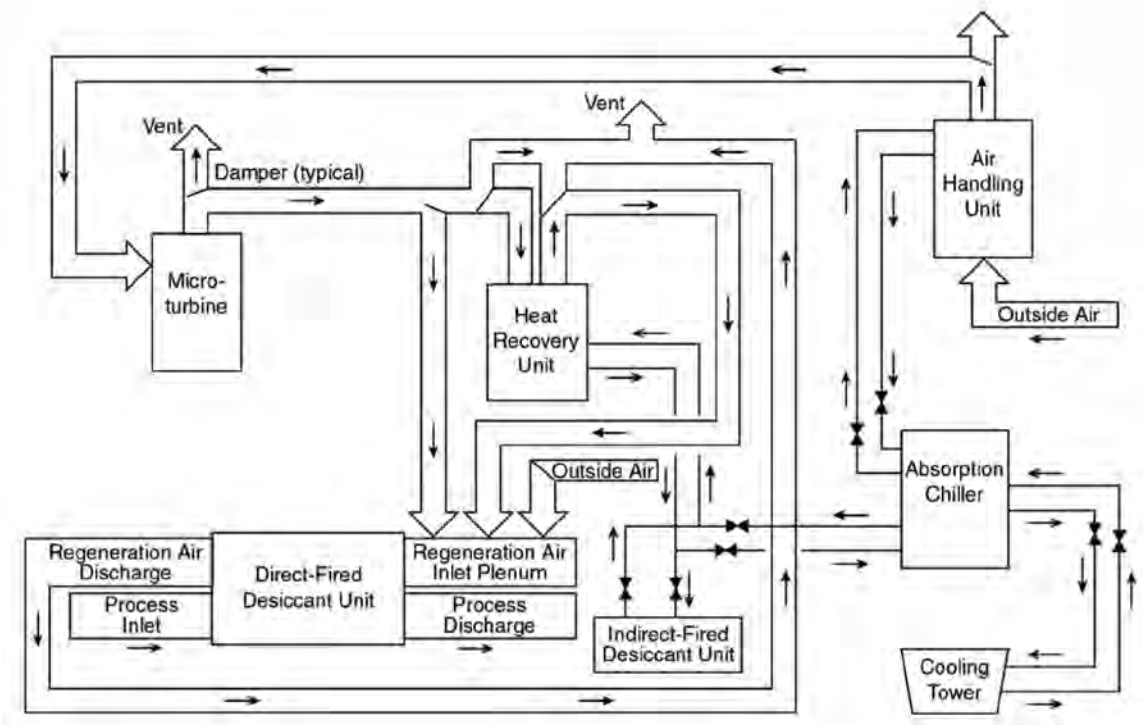

Fig. 1. Schematic of CHP Integrated Test Facility at ORNL. (*Source:* "DER Performance Testing of a Microturbine-Based Combined Cooling, Heating, and Power (CHP) System PERFORMANCE," Proceedings of Power System 2002 Conference, Clemson, SC, March 2002).

recovery unit (HRU), an indirect-fired, single-effect, 10-ton absorption chiller (ABSC), and direct-fired (DFDD) and indirect-fired (IFDD) desiccant dehumidifiers. Under normal conditions, the heated air or hot water input for these TATs is generated by natural gas firing. In the CHP configuration, the waste exhaust heat from the gas-fired microturbine provides the thermal energy input.[1,2]

The microturbine exhaust gas, at a temperature normally ranging from 250 to 293°C (482 to 560°F), can be directed through different paths depending on the configuration to be tested. Hot water ranging in temperature from 85 to 95°C (185 to 203°F) can be generated by directing the microturbine exhaust gas through an exhaust-gas-to-liquid heat exchanger (e.g., an HRU). The hot water generated in the HRU can be input to either an indirect-fired desiccant dehumidification system or a 10-ton, indirect-fired, single-effect absorption chiller. The temperature of the exhaust gas leaving the HRU is ~120°C (~248°F). For testing a direct-fired desiccant system, the exhaust gas can be supplied directly to the desiccant system inlet plenum or passed through the HRU to generate hot water and then be directed to the direct-fired desiccant system inlet plenum.[1,2]

2.2 TEST FACILITY COMPONENTS[1,2]

2.2.1 Microturbine

The microturbine, a three-phase 480-VAC/30-kW-rated unit, is designed to operate at a maximum speed of 96,000 rpm, generate 50 or 60 Hz power, produce a continuous phase current of 36 A at 480 VAC, and a near unity power factor when the unit is grid connected. The unit's nominal phase-to-neutral voltage is 277 VAC. The power-conditioning electronics of the turbine generator rectifies the high-frequency ac power from the generator to constant-voltage DC power, which is then inverted to 50 or 60-Hz constant-frequency ac power.[1,2]

The microturbine's natural gas fuel is supplied by the gas distributor at a pressure of only 0.3 atm (5 psig) and the unit requires natural gas at a pressure of 3.7 atm (55 psig); therefore, a gas compressor is used to increase the pressure before it enters the microturbine combustion chamber. An exhaust-gas-to-air heat exchanger/recuperator is used to preheat the air entering the combustion chamber, improving the electrical efficiency of the microturbine by ~10% from 13 to 23% based on the higher heating value (HHV) of the natural gas.

2.2.2 Heat Recovery Unit[3–6]

The HRU, an exhaust-gas-to-liquid heat exchanger, is used to recover a portion of the waste heat in the microturbine exhaust gas and produce hot water for heating, input to the IFDD system, or input to the absorption chiller. Although the HRU nominal water flow rate is ~4.3 m^3/h (~19 gpm), CHP system configuration tests were performed with water flow rates as high as ~9 m^3/h (~39.8 gpm). At a water flow rate of ~5.8 m^3/h (~26 gpm) the maximum water temperature is ~91°C (~196°F). Actual water temperature depends on several parameters, such as microturbine power output, ambient temperature, and HRU water flow rate. The exhaust gas leaving the HRU has sufficient waste heat to potentially provide the thermal input to additional direct-fired TATs, such as a direct-fired desiccant dehumidification unit (DFDD).

2.2.3 Desiccant Dehumidifiers[1,2,4,5,7]

Desiccant dehumidifiers provide an alternative to mechanical refrigeration for removing moisture from air before it enters a conditioned space. The desiccant material attracts water from the air as a vapor rather than condensed liquid. The water vapor pressure difference between humid air (high vapor pressure) and dry desiccant (low vapor pressure) provides the potential that causes water molecule migration from the humid air to the desiccant.

The desiccant dehumidifiers use a wheel of desiccant material mounted between two air streams—a process stream and a reactivation stream. As the wheel rotates between the two air streams, moisture is absorbed from the process stream to nearly saturate the desiccant, and the reactivation stream dries out the desiccant. Moisture released from the desiccant wheel is carried by the reactivation stream and discharged out of the building.

Desiccant units that use heated reactivation air are called "active" to distinguish them from units that use dry building exhaust air for regeneration, which are called "passive." The units in the Integrated Test Facility are active units that can be further classified as "direct-fired" or "indirect-fired," depending on the method used to heat the regeneration air. In a direct-fired unit, natural gas combustion or other heat sources are used to directly heat the regeneration air as shown in Fig. 2. For the direct-fired unit tested in the Integrated Test Facility, hot exhaust from the microturbine mixed with outside air was used for regeneration air.

When an indirect method, such as a hot water or steam-to-air heat exchanger,

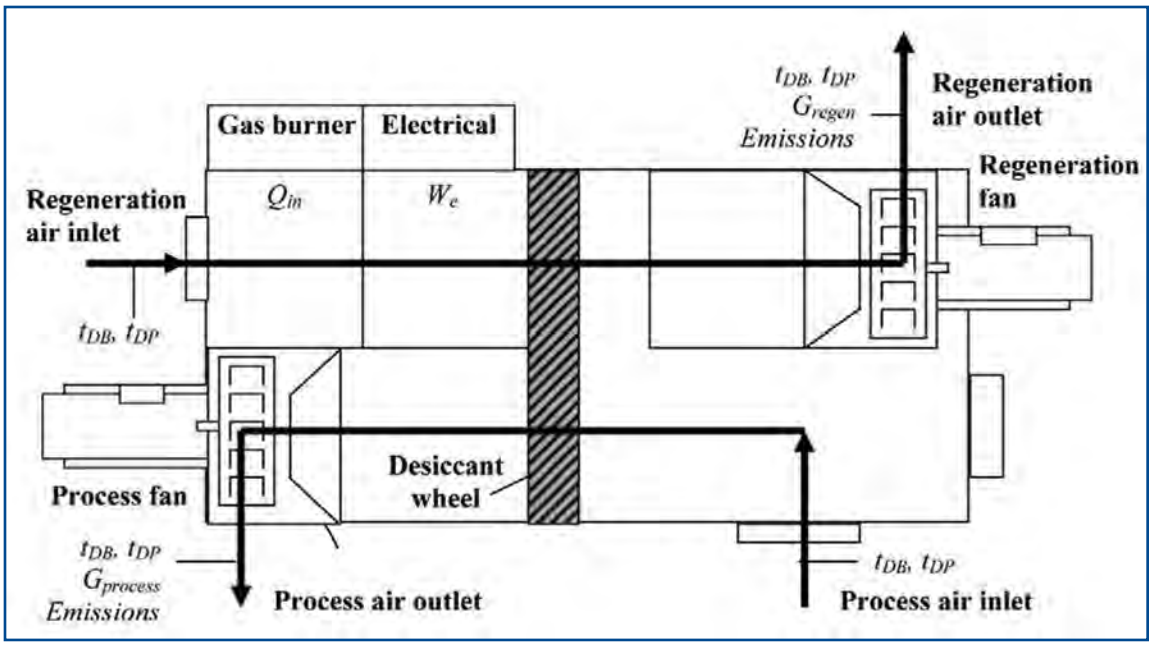

Fig. 2. Schematic of direct-fired desiccant dehumidification unit. (*Source:* "Baseline and IES Performance of a Direct-Fired Desiccant Dehumidification Unit under Various Environmental Conditions," 2003 ASHRAE Transactions of the Annual Meeting, KC-03-5-2, Kansas City, MI, June 2003.)

is used to heat the regeneration air, the unit is classified as an indirect-fired desiccant dehumidification unit. A schematic of an indirect-fired unit is shown in Fig. 3.

The major difference between the IFDD and DFDD units is in the method used to provide the heat necessary to regenerate the desiccant material. In the IFDD the gas burner used to provide heat for regeneration is replaced by a hot water or steam heating coil. As with the DFDD unit, the IFDD has two air streams—regeneration and process. The process return air enters the unit and passes through a desiccant material where heat is added, raising the air temperature and removing moisture[1]. After leaving the desiccant material, the process air flows through a heat recovery wheel where heat is removed and transferred to the regeneration air, decreasing the amount of thermal energy required to raise it to the regeneration temperature.

The regeneration air (outside air) enters the unit and passes through the heat recovery wheel, picking up heat from the process air. After leaving the heat recovery wheel, the regeneration air flows through the regenerative heating coil where it picks up additional heat before passing to the desiccant wheel to remove the absorbed moisture. The regeneration air is then discharged to the atmosphere.

In the Integrated Test Facility, indirect-fired testing configuration hot water generated by heat recovered through the HRU and a hot-water-to-air heat exchanger were used to heat the reactivation air.

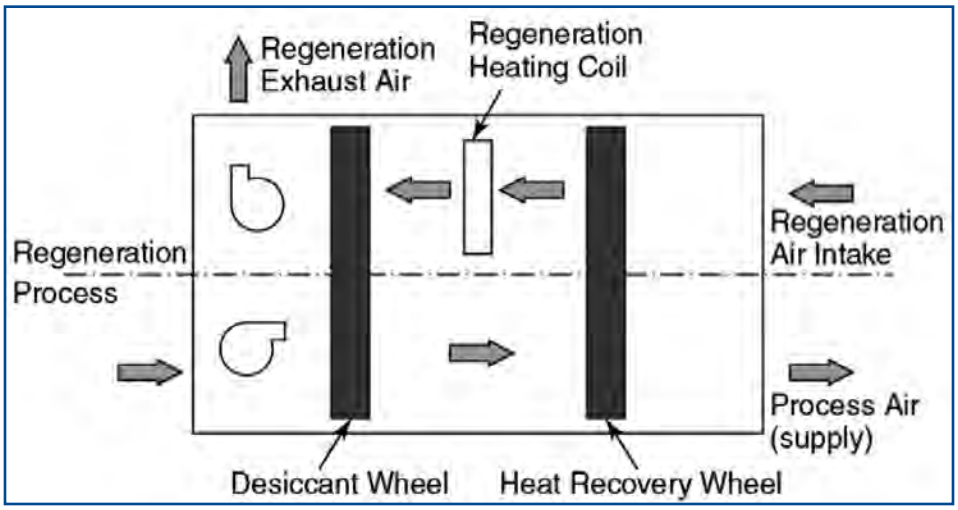

Fig. 3. Schematic of indirect-fired desiccant dehumidification unit. (*Source:* "CHP Integration (OR IES): Maximizing the Efficiency of Distributed Generation with Waste Heat Recovery," Proceedings of the power Systems 2003 Conference, Clemson, SC, March 2003.)

2.2.4 Absorption Chiller[8]

Absorption chillers generate chilled water (~44°F or ~7°C) from a heat source as opposed to mechanical compression of vapor. Water-lithium-bromide absorption chillers using water as the refrigerant and lithium-bromide as the

absorbent are classified by the method of heat input (direct-fired or indirect-fired) and whether the absorption cycle is single or multiple effect. The direct-fired absorption chillers contain fossil fuel burners to provide the heat source. Indirect-fired units use hot water or steam from a separate heat source to provide the heat input. Exhaust-fired unites use hot exhaust gases directly as their heat source.

Single-effect absorption chillers generally use water from 116°C to132°C (240°F to 270°F) with some smaller machines for waste heat applications using 190°F, or low pressure (9 to 12 psig) steam. Double-effect chillers provide increased efficiency but also need higher-pressure steam (i.e., 100 psig) or high-temperature water (i.e., 188°C or 370°F). The current CHP test facility configuration contains an indirect-fired, single-effect 10-ton AC.

2.3 EMISSIONS MONITORING[7]

The air pollutants most significant to gas microturbine-based CHP system operation are nitrogen dioxide (NO_2), carbon monoxide (CO), and sulfur dioxide (SO_2), all of which can have a significant effect on the level of environmental pollution. These pollutants along with, lead (Pb), ozone (O3), and particulates are among six criteria air pollutants that have had ambient air limits set by the U.S. Environmental Protection Agency. Therefore, these three pollutants were of most interest during the emissions studies performed at the Integrated Test Facility.

An Enerac 3000E flue gas analyzer supported by Enercom 2000 software and electrochemical sensor was used for emissions monitoring of the microturbine flue gas. The concentrations of NOx, CO, and SO2 were measured in ppm by volume (i.e., volume of gaseous pollutant per million volumes of ambient air) at the test oxygen concentration, corrected to 15% O2 (typical requirement for comparison of various DG equipment) and then converted to mg/m^3.

3. MICROTURBINE BASELINE CHARACTERIZATION[1,2]

The first phase of testing the 30-kW microturbine and CHP consisted of characterizing the baseline performance of the microturbine. The collected electrical data included the microturbine's DC voltage, and single- and three-phase power output, voltage, and current. The thermal data included the microturbine's input temperature, exhaust temperature, internal temperatures at the compressor and turbine, and emissions.

The baseline characterization tests were performed without TATs connected to the microturbine exhaust. Even without the presence of any equipment for thermal recovery, some degree of backpressure exists (~8.0×10^{-4} atm or 0.3 in wc), although this is quite low. The effect of exhaust back pressure on the microturbine's power and efficiency is discussed in Sect. 4.0.

3.1 STARTUP, SHUTDOWN, AND DISPATCH CHARACTERISTICS[1,2]

The startup, shutdown, and power dispatch characteristics (power output and speed) of the microturbine are shown in Figs. 4–6. Startup in this case is defined as 0 rpm and 0 power output to operating speed and full output power generation.

As shown in Fig. 4, startup requires ~200 s. During the initial ~40 s of turbine warm-up, auxiliary power (~2 kW) is provided by the grid, which is shown as negative power output in Fig. 4. The microturbine controls maintain the microturbine speed at ~25,000 rpm until the microturbine begins to generate power and then at ~45,000 rpm for ~115 s during the remainder of the warm-up cycle. After the warm-up period, the microturbine controls increase the speed to obtain the desired startup output power setting. This characteristic is basically the same regardless of the power output setting for startup.

Shutdown, shown in Fig. 5, requires 520 s. Most of this time, ~475 s, is required to cool down the turbine. Although the power output dropped off fairly linearly, the turbine speed stayed at 45,000 rpm for nearly all the shutdown time.

The power dispatching characteristics are shown in Fig. 6. It was found that it took ~20 s to vary the microturbine's power output. Figure 6 shows the transition time from ~10 kW to ~30 kW.

3.2 POWER OUTPUT VARIATION

The variability of the microturbine's power output at the full power setting (30 kW) over a one-hour period is shown in Fig. 7.[2]

3.3 PERFORMANCE AT VARIOUS POWER SETTINGS[2]

To characterize the microturbine's performance at various power settings, tests were performed at power settings ranging from full output (30 kW) to one-sixth power (5 kW) in 5-kW

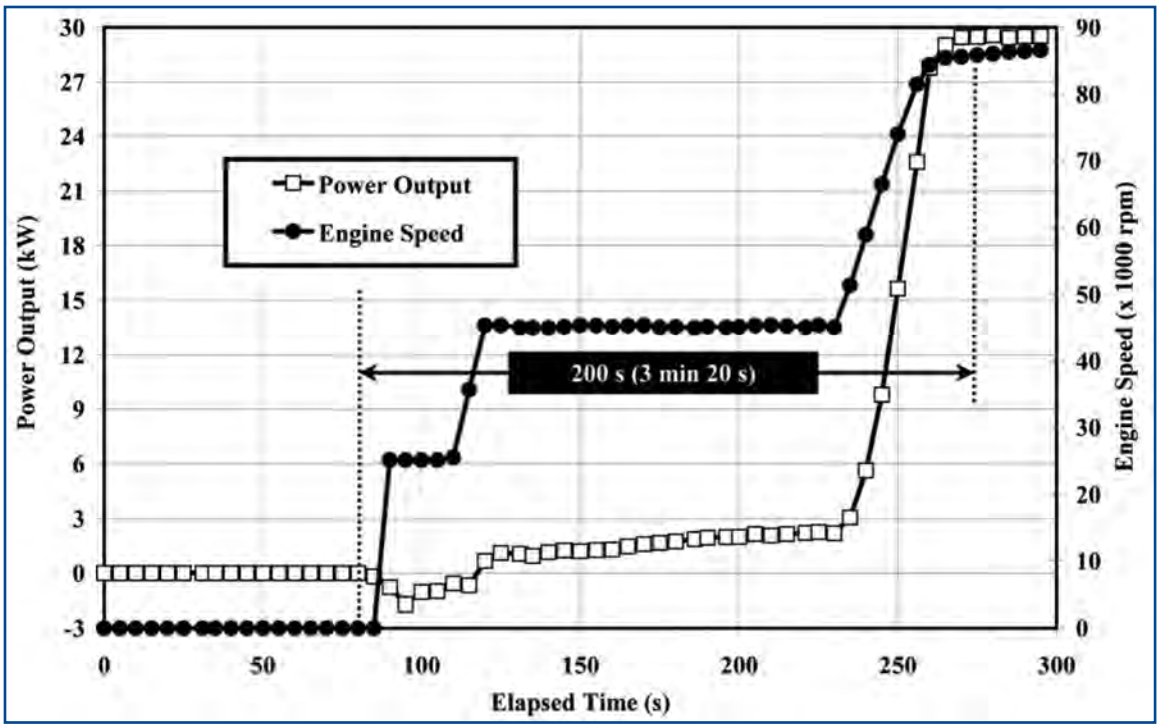

Fig. 4. Startup power output and turbine speed. (*Source:* "DER Performance Testing of a Microturbine-Based Combined Cooling, Heating, and Power (CHP) System," Proceedings of Power System 2002 Conference, Clemson, SC, March 2002.

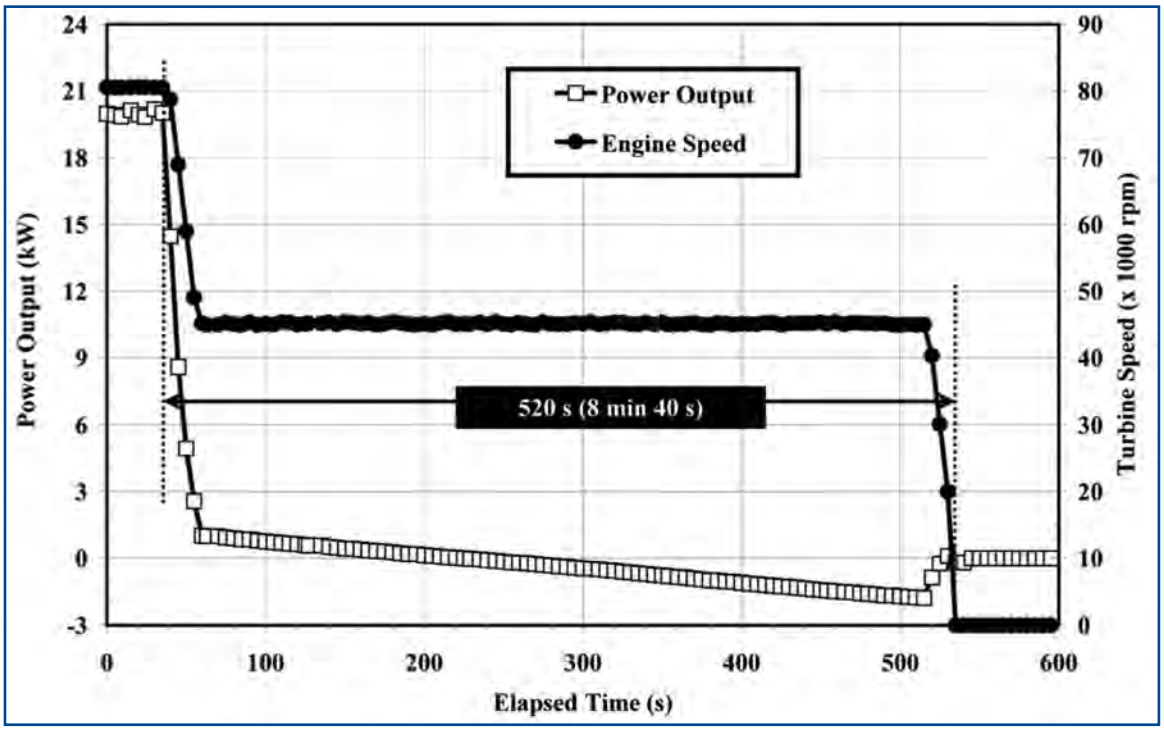

Fig. 5. Shutdown power output and turbine speed. (*Source:* "DER Performance Testing of a Microturbine-Based Combined Cooling, Heating, and Power (CHP) System," Proceedings of Power System 2002 Conference, Clemson, SC, March 2002.

increments. The results are presented in Table 1, which contains the microturbine's power setting, measured power output, turbine speed, phase voltages and currents (a, b, and c), and rectified dc voltage and standard deviations for some of these values. It should be noted that the outdoor temperatures were below the ISO temperature of 15°C (59°F) that is the typical rating condition for microturbines. The measured emissions at the various power settings are also presented. Emission characteristics are discussed in Sect. 6.

In the grid-dependent (grid-connected) mode, for a power output range of 30 to 20 kW, the microturbine was found to operate at a power factor of 98% with a ±0.86% standard deviation; and for power output range of 15 to 5 kW, generated at 97% with a standard deviation of ±0.80%.

The data in Table 1 show that the unit's efficiency decreases with the power output level. At the full power setting of 30kW, the microturbine can produce ~28 kW at an

efficiency of ~23%. At an output power setting of 5 kW, the microturbine has an efficiency of only ~12%. The microturbine's exhaust temperature varied from ~264°C (~508°F) at the unit's maximum power demand setting (30 kW) to ~196°C (~384°F) at the minimum power setting of 5 kW. The energy efficiency and exhaust temperature of the microturbine as they vary with power output are shown in Fig. 8.

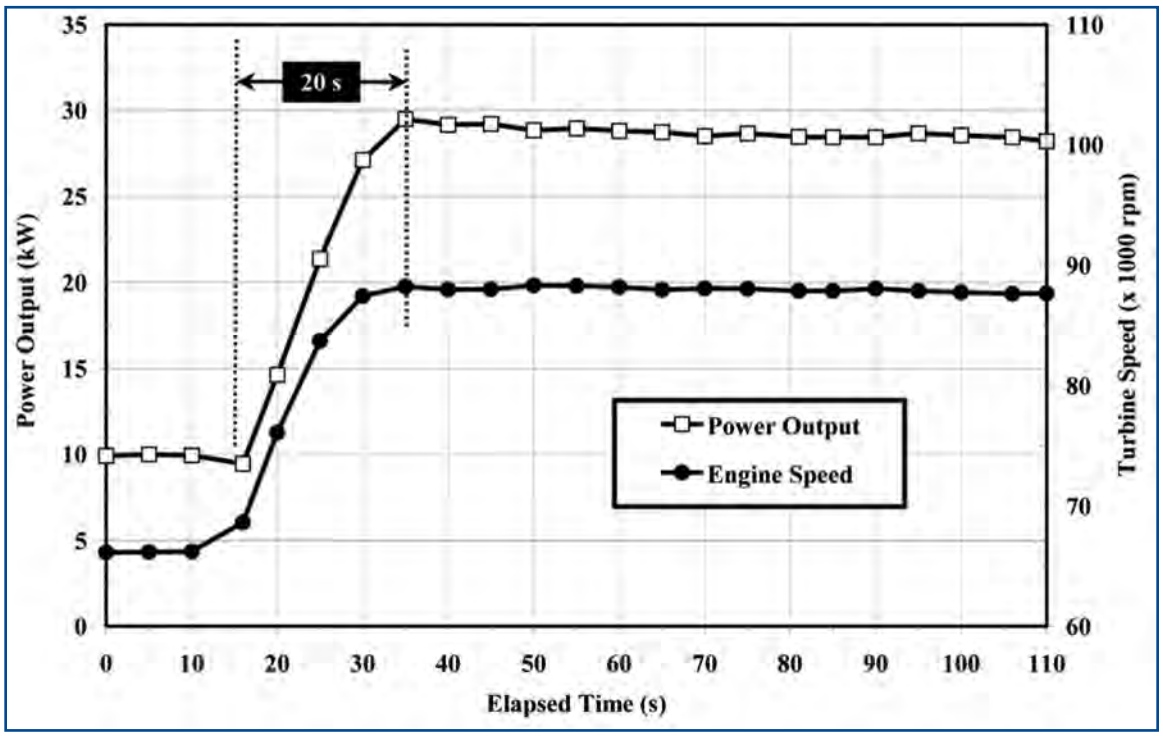

Fig. 6. Power dispatching response: power output and turbine speed. (*Source:* "DER Performance Testing of a Microturbine-Based Combined Cooling, Heating, and Power (CHP) System," Proceedings of Power System 2002 Conference, Clemson, SC, March 2002.

3.4 EFFECT OF AMBIENT TEMPERATURE ON ACHIEVABLE POWER OUTPUT AND EXHAUST TEMPERATURE[4]

One of the factors affecting the performance of the turbine is the ambient air mass flow. Since a turbine is a fixed-displacement machine, the air mass flow is a direct function of the ambient air density, which in turn is a function of the ambient air temperature and humidity. The tested microturbine generator (MTG) controls the net power output by

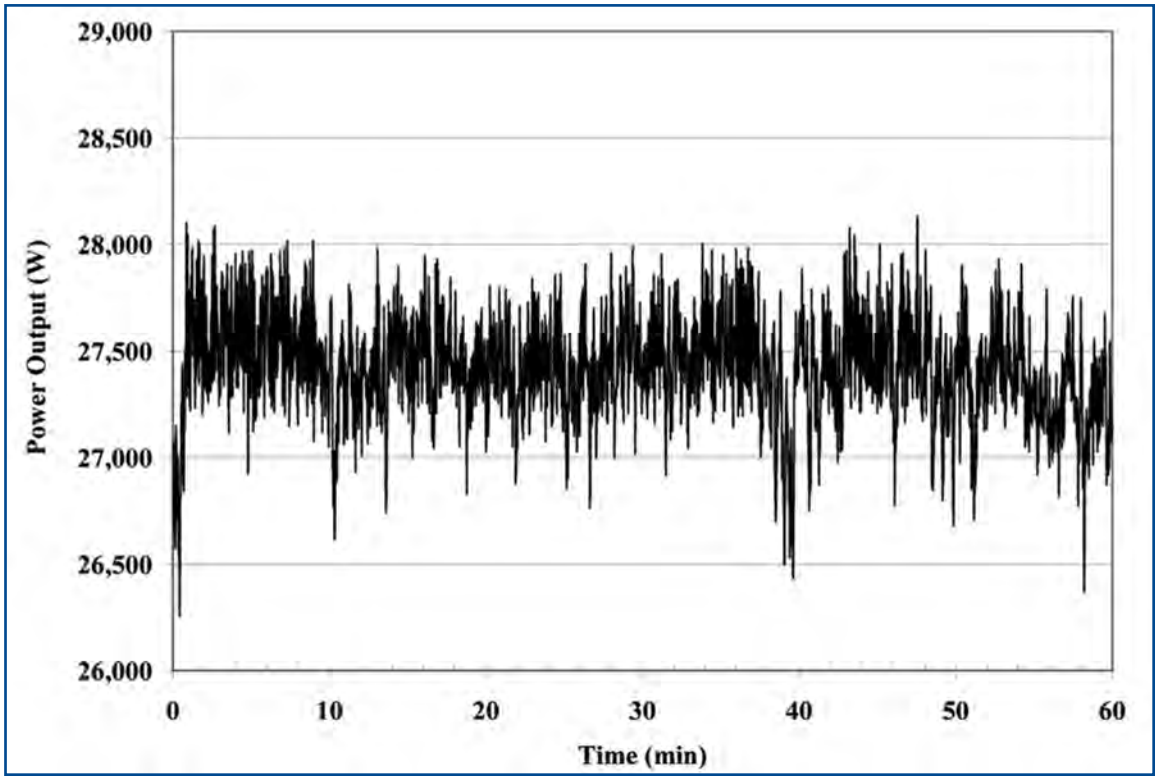

Fig. 7. Microturbine power output variation for 1 h at 30 kW. (*Source:* "Integration of Distributed Energy Resources and Thermally-Activated Technologies," DistribuTech Conference, Miami Beach, FL, February 2002.)

Table 1. Microturbine performance characteristics at various power settings (Ref. 2)

Power Setting (kW)	Power output (W)	% Efficiency (HHV)[8]	$T_{exhaust}$ (°F)	Engine speed (RPM)	DC Voltage (V_{dc})	Phase Voltage (V_{rms})	Phase Current (A_{rms})	CO** (ppm)	NO_x** (ppm)	CO_2 (%)	O_2 (%)
30	27421 ± 237	22.57 ± 0.06	507.5 ± 0.6	91,735 ± 159	759.7 ±0.4	289.0 286.8 286.9	32.0 32.0 32.0	16	4	1.5	18.5
25	24658 ± 187	22.15 ± 0.14	493.2 ± 0.7	88,496 ± 175	759.7 ±0.4	289.3 286.9 287.1	28.3 28.3 28.1	51	3	1.4	18.5
20	19775 ± 189	21.63 ± 0.07	471.8 ± 0.6	81,796 ± 116	759.6 ±0.4	287.3 285.1 285.4	23.0 23.0 23.0	68	3	1.3	18.7
15	14792 ± 146	20.47 ± 0.06	443.5 ± 0.5	74,928 ± 123	759.9 ±0.5	287.0 284.9 285.2	17.0 17.0 17.0	5	35	1.2	18.9
10	9785 ± 101	17.51 ± 0.08	419.4 ± 0.3	67,684 ± 72	759.6 ±0.2	286.1 284.2 284.4	11.1 11.0 11.0	10	30	1.1	19.1
5	4,982 ± 84	12.34 ± 0.07	384.2 ± 1.0	57,793 ± 84	759.5 ±0.0	284.4 282.5 282.6	6.0 6.0 6.0	22	22	1.1	19.2

**All performance measurements were taken at similar outside temperature conditions, between 39°F (3.9°C) and 34°F (1.1°C). Sixty-eight percent or more of the measurements fall within one standard deviation, which is shown as the ± range. **Actual CO and NO_x measurements are shown and have not been corrected to 15% O_2.*

adjusting the turbine speed to achieve the desired power output setting at the given ambient temperature. The maximum speed allowed by the MTG controller is 96,000 rpm, which limits possible temperature compensation. At a given ambient temperature when the maximum turbine speed limit is reached for a specific power output setting, it is not possible to compensate for any further increases in ambient temperature. Therefore the net power output of the MTG decreases as the ambient temperature increases, and the desired power output setting cannot be achieved.

For the tested microturbine, the maximum speed limit was found to affect only the 30-kW and 25-kW power settings. As can be seen in Fig. 9, at the 30-kW and 25-kW output settings the critical ambient temperature is ~13°C (~56°F) and ~21°C (~70°F), respectively.

The effect of ambient air temperature on exhaust gas temperature is shown in Fig. 10: exhaust gas temperature increases with the rise in ambient air temperature. After the critical temperature is reached, the exhaust gas temperature continues to increase with increased ambient temperature, but at a lower rate.[6]

4. BACK-PRESSURE TESTS[1–3]

For a turbine-only configuration, the back-pressure (i.e., pressure at the turbines exhaust outlet) consists of the pressure drop through the exhaust stack and silencers. Heat recovery equipment interfaced with a turbine increases the back-pressure and reduces the power output. The objective of this test was to investigate the dependence of the microturbine's power and efficiency on the exhaust back-pressure.

Two series of back-pressure tests were performed; one at constant output power demand and another at constant engine speed. In each series of tests, the total power output demand of the microturbine was varied in increments of 5 kW from 10 kW to 30 kW. The back-pressure on the unit was adjusted by a slide damper in the exhaust duct, as shown in Fig. 11. Constant output power demand tests were performed with the damper in three different

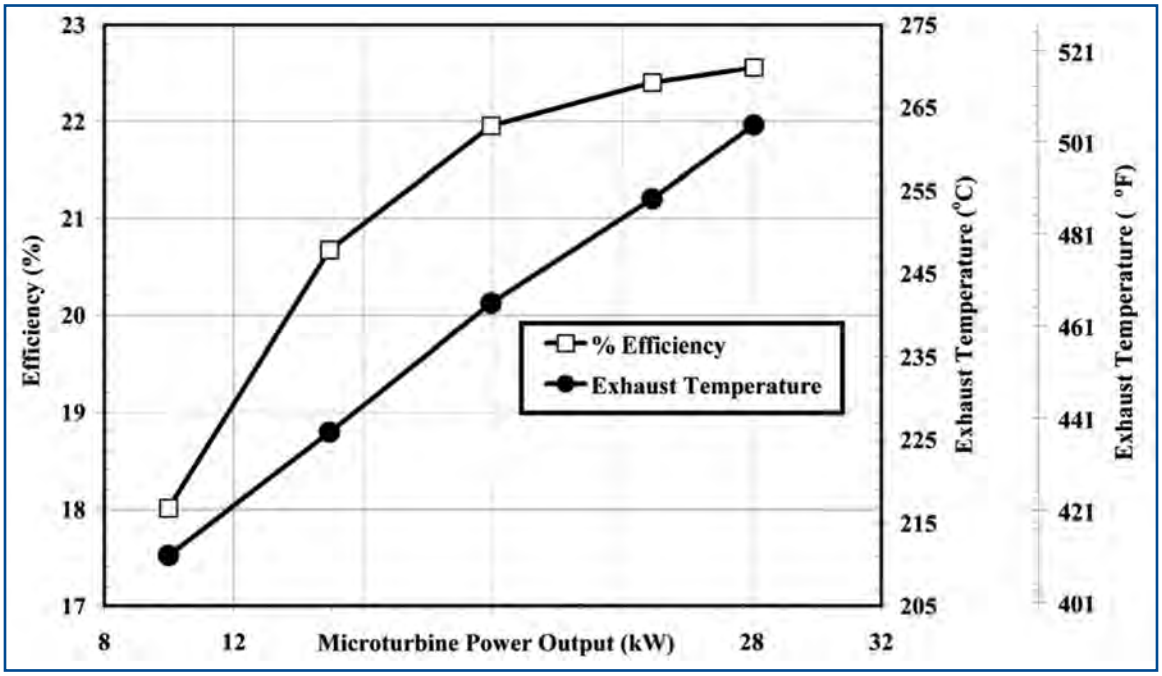

Fig. 8. Efficiency and exhaust temperature versus power output. (*Source:* "Integration of Distributed Energy Resources and Thermally-Activated Technologies," DistribuTech Conference, Miami Beach, FL, February 2002.)

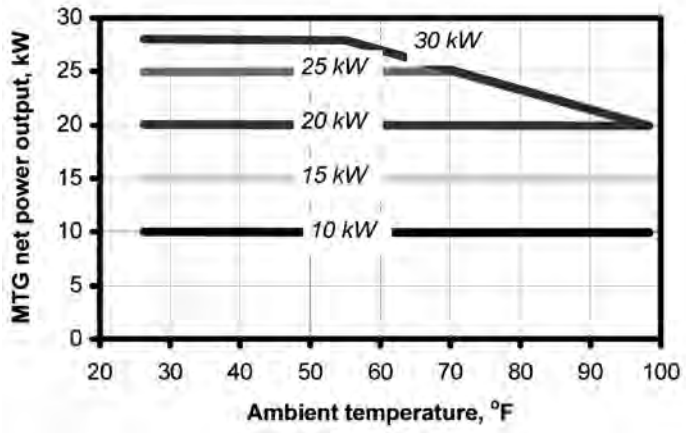

Fig. 9. Effect of ambient temperature on power output. (*Source:* "CHP Integration (OR IES): Maximizing the Efficiency of Distributed Generation with Waste Heat Recovery," Proceedings of the Power Systems 2003 Conference, Clemson, SC, March 2003.)

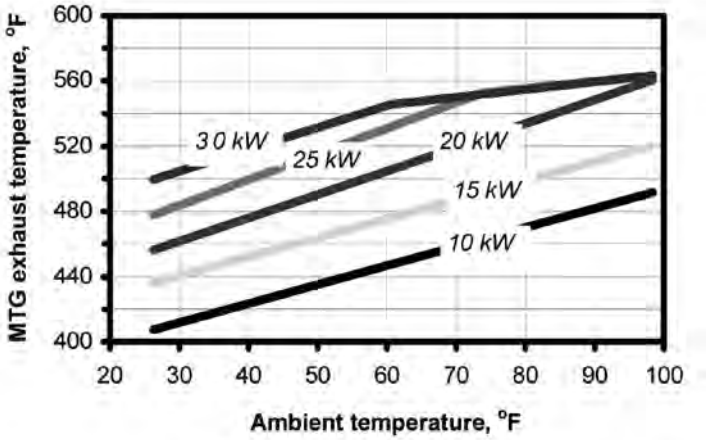

Fig. 10. Effect of ambient temperature on exhaust temperature. (*Source:* "CHP Integration (OR IES): Maximizing the Efficiency of Distributed Generation with Waste Heat Recovery," Proceedings of the Power Systems 2003 Conference, Clemson, SC, March, 2003.)

positions—fully open, 1/4 closed, and 3/8 closed—and for the constant engine speed tests, the slide damper was varied over five settings. In both tests, the back-pressure was monitored by a pressure transducer also located in the exhaust duct.

Because the microturbine was located outdoors, the microturbine's air inlet temperature was dictated by outdoor conditions.

4.1 CONSTANT POWER OUTPUT DEMAND

Tests were conducted at various power output demands and microturbine back-pressures (damper at three different positions of fully open, 1/4 closed, and 3/8 closed). At full power demand, the

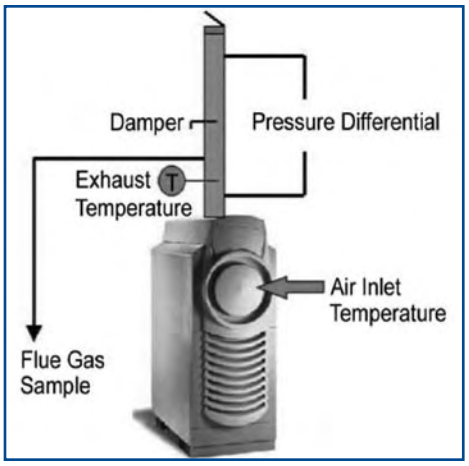

Fig. 11. Experimental setup for baseline testing microturbine. (*Source:* "Experimental and Theoretical Study of Gas Micro-turbine-Based BCHP System," Proceedings of the 2001 ASME International Mechanical Engineering Congress and Exposition, AES-23622, New York, NY, November 2001.)

back pressure varied from 8.34×10^{-4} atm to 1.8×10^{-2} atm (0.34 to 7.34 in. water column). During these tests, the microturbine's controller adjusted the engine speed to match the power demand setting as closely as possible with or without the back-pressure. The results for damper at the full open and 3/8 closed positions are presented in Tables 2 and 3, respectively.

The turbine inlet air temperature is not controlled but dictated by ambient temperature and, as noted in Sect. 3.4, the turbine speed is increased to compensate for increases in ambient temperature. Therefore, the rpm increase observed between Tables 2 and 3 is dependent on both increased ambient temperature and increased back-pressure. Since the engine speed could adjust and compensate for the back pressure and ambient temperature increases, the power output and efficiency at corresponding output power demands were not significantly affected.

In order to show the reproducibility of the measured data, the tests with the damper fully open were repeated for the power demand setting of 20 kW. The observed relative power output and efficiency percentage differences were less than 0.3%.

4.2 CONSTANT ENGINE SPEED

Another series of tests were conducted while the microturbine was maintained at approximately constant engine speed and the back-pressure was varied for each nominal power output. Table 4 shows the results at full power demand of 30 kW only. At the full power demand and approximately constant engine speed, as the back-pressure was increased from approximately 8.00×10^{-4} to 1.72×10^{-2} atm (0.33 to 6.99 in. water column), the average turbine efficiency dropped by less than 2%, and the average turbine power output decreased by less than 6% of the values with damper fully open.

5. HEAT RECOVERY AND CHP EFFICIENCY

On-site distributed generation (DG), as part of an integrated energy system (IES), allows the waste heat from fuel-fired DG sources to be used to meet the end user's thermal loads and substantially improve overall system energy efficiency and fuel economy. As discussed in Sect. 1, the IES Test Laboratory at ORNL allows configuration of DG with various heat recovery units (presently an air-to-water HRU, direct- and indirect-fired desiccant dehumidification systems, and an indirect-fired, single-effect absorption chiller) in order to test the

Table 2. Capstone 30-kW microturbine with damper fully open (Ref. 3)

Power demand setting (W)	Power output (W)	Efficiency (HHV)*	$T_{air\ inlet}$ (°F)	$T_{exhaust}$ (°F)	Engine speed (RPM)	ΔP (in. wc)	NO (ppm)	NO_x (ppm)	CO_2 (%)	CO (ppm)	O_2 (%)	Voltage phases A, B, C (V)
30000	27678 ± 135	0.2313 ± 0.0011	27.6 ± 1.2	494.4 ± 0.5	88980 ± 183	0.34 ± 0.09	0	0	1.4	16	18.5	289, 288, 288
25000	24963 ± 87	0.2265 ± 0.0008	29.3 ± 0.9	484.0 ± 0.4	86048 ± 135	0.28 ± 0.07	0	0	1.4	33	18.6	289, 288, 288
20000	19987 ± 110	0.2178 ± 0.0012	29.2 ± 0.9	457.9 ± 0.6	80377 ± 131	0.23 ± 0.07	0	0	1.3	130	18.7	287, 286, 285
20000	20037 ± 97	0.2172 ± 0.0011	33.7 ± 0.5	463.0 ± 0.3	81264 ± 60	0.22 ± 0.05	0	0	1.3	127	18.7	289, 287, 287
15000	15040 ± 86	0.2044 ± 0.0012	35.4 ± 0.7	437.3 ± 0.4	75076 ± 69	0.16 ± 0.05	24	24	1.2	10	18.9	287, 286, 285
10000	9994 ± 71	0.1798 ± 0.0013	35.4 ± 0.8	407.7 ± 0.5	67461 ± 87	0.11 ± 0.04	19	19	1.1	17	19.1	286, 285, 284

*Efficiency is based on natural gas higher heating value.

Table 3. Capstone 30-kW microturbine with damper 3/8 open (Ref. 3)

Power demand setting (W)	Power output (W)	Efficiency (HHV)*	$T_{air\ inlet}$ (°F)	$T_{exhaust}$ (°F)	Engine speed (RPM)	ΔP (in. wc)	NO (ppm)	NO_x (ppm)	CO_2 (%)	CO (ppm)	O_2 (%)	Voltage phases A,B,C (V)
30000	28646 ± 235	0.2256 ± 0.0019	37.9 ± 1.6	517.2 ± 1.8	92956 ± 365	7.34 ± 0.17	0	0	1.4	11	18.5	290, 289, 288
25000	25031 ± 85	0.2212 ± 0.0008	40.1 ± 0.9	500.3 ± 0.9	88772 ± 162	6.14 ± 0.10	0	0	1.4	43	18.5	289, 288, 287
20000	19941 ± 131	0.2123 ± 0.0014	41.1 ± 0.9	473.5 ± 0.7	82688 ± 113	4.57 ± 0.09	0	0	1.3	134	18.7	288, 287, 286
15000	14993 ± 90	0.2007 ± 0.0012	41.3 ± 0.7	445.6 ± 0.5	76194 ± 95	3.37 ± 0.09	25	25	1.2	6	18.9	286, 285, 285
10000	9965 ± 58	0.1769 ± 0.0010	41.2 ± 0.4	415.0 ± 0.3	68383 ± 51	2.28 ± 0.04	19	19	1.1	17	19.1	285, 284, 284

*Efficiency is based on natural gas higher heating value.

Table 4. Microturbine performance at constant speed and varying back-pressure (Ref. 3)

Power output (W)	Efficiency (HHV)*	$T_{air\ inlet}$ (°F)	$T_{exhaust}$ (°F)	Engine speed (RPM)	ΔP (in. wc)	NO (ppm)	NO_x (ppm)	CO_2 (%)	CO (ppm)	O_2 (%)	Voltage phases A,B,C (V)
28064 ± 142	0.2256 ± 0.0011	34.3 ± 1.5	505.2 ± 1.5	90504 ± 252	0.33 ± 0.09	0	0	1.3	19	18.8	288, 287, 287
27926 ± 147	0.2269 ± 0.0012	32.6 ± 1.7	504.9 ± 1.3	90799 ± 271	0.34 ± 0.09	0	0	1.5	14	18.5	288, 287, 286
27984 ± 139	0.2269 ± 0.0011	31.6 ± 1.4	504.0 ± 1.1	90867 ± 306	1.88 ± 0.09	0	0	1.5	14	18.5	288, 287, 286
27594 ± 152	0.2248 ± 0.0012	33.9 ± 1.6	506.1 ± 1.6	90902 ± 296	4.50 ± 0.17	0	0	1.5	17	18.4	289, 288, 287
26884 ± 182	0.2226 ± 0.0015	38.4 ± 1.7	508.0 ± 0.9	91055 ± 281	5.78 ± 0.16	0	0	1.5	28	18.5	288, 287, 286
26489 ± 133	0.2213 ± 0.0011	39.8 ± 1.5	508.9 ± 1.4	90974 ± 292	6.99 ± 0.13	0	0	1.4	31	18.5	288, 287, 287

*Efficiency is based on natural gas higher heating value.

component and overall IES performance. The following sections discuss results of tests performed at the ORNL IES Laboratory for configurations of a 30-kW microturbine DG source, an HRU, and various thermally activated technologies.

5.1 AIR-TO-WATER HEAT EXCHANGER (e.g., HRU)[1,2]

Since all of the thermally activated technologies were tested with the HRU as a part of the IES, the first tests to be discussed are for the MTG and exhaust-gas-driven, air-to-water heat exchanger HRU. These tests were performed to determine the quantity of MTG waste heat that could be recovered to generate hot water for space heating or use with other thermally activated technologies and to determine the IES (MTG + HRU) efficiency, both as a function of microturbine output power. The HRU water flow rate for this series of tests was 4.3 m^3/h (19 gpm), and the power output of the turbine was varied from 10 to 30 kW in increments of 5 kW.

The resulting recoverable waste heat was found to be ~23 kW (~75,000 Btu/h) with the microturbine at one-third power up to ~ 44 kW (or~150,000 Btu/h) with the unit at full power as shown in Fig. 12. The measured exhaust flue gas temperature rejected to the atmosphere (leaving the heat exchanger) was ~127°C (260°F) at full power; however, at one-third power the exhaust temperature was ~93°C (200°F).

Figure 13 shows a relatively constant measured IES system (measured CHP) efficiency of ~55% based on a higher heating value (HHV) for the natural gas over the microturbine's power output range. For comparison purposes, the microturbine efficiency without heat recovery (microturbine), which ranges from approximately 18 to 24%, and the manufacturer's data are also shown in Fig. 13. The test efficiency agreed well with the published performance data.

5.2 DESICCANT DEHUMIDIFICATION[4,5]

Tests were conducted at the ORNL IES Laboratory Facility for IES configurations employing a commercially available direct-fired desiccant dehumidification

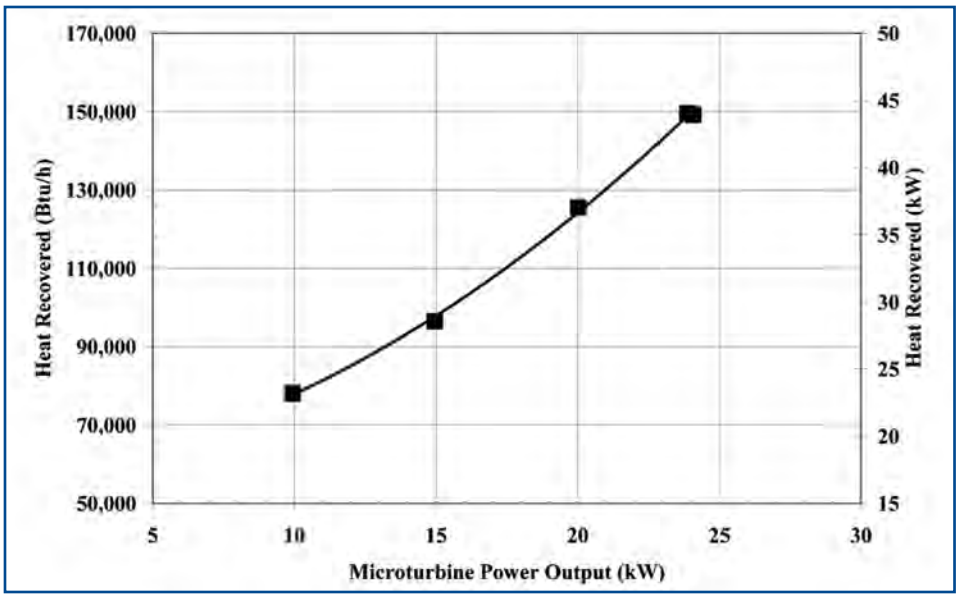

Fig. 12. Heat recovery by the HRU at a water flow rate of 4.3 m3/h (19 gpm). (*Source:* "Integration of Distributed Energy Resources and Thermally-Activated Technologies," DistribuTech Conference, Miami Beach, FL, February 2002.)

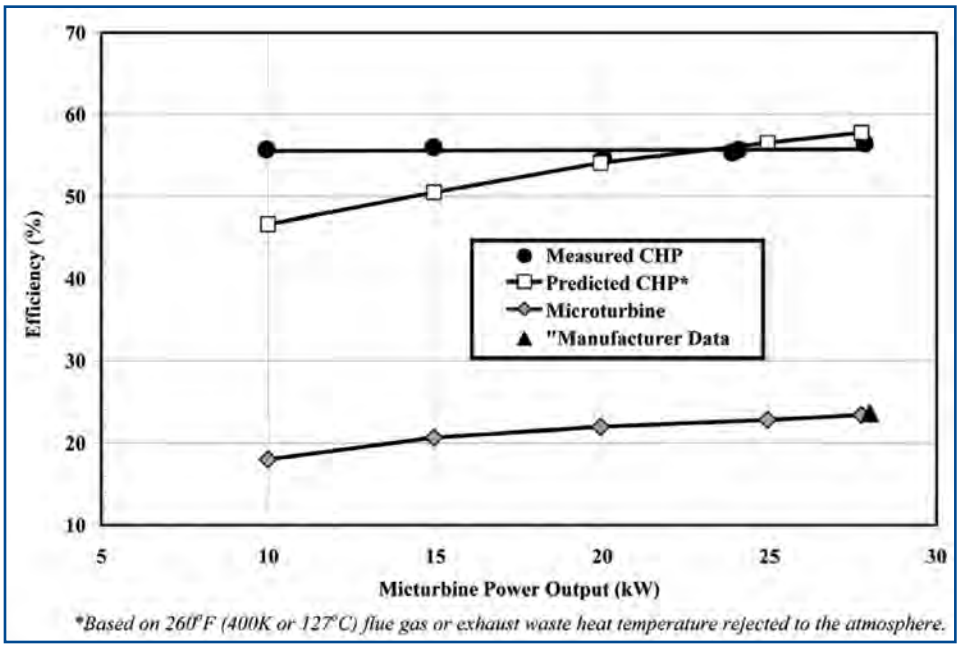

Fig. 13. IES system and microturbine: heat recovery efficiencies. (*Source:* "Integration of Distributed Energy Resources and Thermally-Activated Technologies," DistribuTech Conference, Miami Beach, FL, February 2002.)

unit and an indirect-fired (hot water) desiccant unit. Both configurations used the 30-kW microturbine as the DG source. These tests investigated the performance of the desiccant dehumidification units as one of the components of an IES. The desiccant unit performance parameters of most interest were the latent capacity (LC) and the latent coefficient of performance (LCOP). The LCOP is a measure of the desiccant dehumidification unit's efficiency and is calculated as the ratio of the LC to the total energy input (thermal + electrical), including the gas input, which is based on HHV of the gas and electrical parasitics (desiccant wheel motor, fans, electronics, etc.). Both configurations are discussed in the following sections.

5.2.1 Direct-Fired Desiccant Dehumidification[4,5]

A commercially available direct-fired desiccant dehumidification unit was used in this series of tests. Test conditions for the process and regenerative inlet dry bulb temperatures were maintained by 10- and 30-kW heaters, and the dew-point temperatures were maintained by injecting steam into the inlet sections of the process and regenerative air streams.

Tests were performed for the baseline configuration, with regeneration air heated by direct burning of natural gas, and an IES configuration, where the exhaust gas from the microturbine was used as the regeneration energy source. In the IES configuration, the gas burner was deactivated. The exhaust gas was passed through the HRU to produce hot water prior to entering the desiccant unit regeneration inlet plenum.

Table 5. Comparison of manufacturer's test data and laboratory results (Ref. 5)

Process inlet test parameters	Process outlet Manufacturer's data				Process outlet Laboratory tests			
	DB °F (°C)	DP °F (°C)	Grains /lb of dry air (/kg of dry air)	LC Btu/h (kW)	DB °F (°C)	DP °F (°C)	Grains /lb of dry air (/kg of dry air)	LC Btu/h (kW)
DB 80°F (26.7°C) WB 67.4°F (19.7°C) DP 61.0°F (16.1°C) Grains 80	119.0 (48.3)	37.5 (3.1)	32.9 (72.5)	80,750.0 (23.6)	116.3 (46.8)	41.5 (5.3)	38.6 (85.1)	80,815.4 (23.7)
DB 85°F (29.4°C) WB 78.1°F (25.6°C) DP 75.8°F (24.3°C) Grains 135	137.0 (58.3)	57.8 (14.3)	71.3 (157.2)	108,460.0 (31.8)	123.9 (51.1)	60.6 (15.9)	79.0 (174.2)	103,246.3 (30.2)
DB 95°F (35.0°C) WB 76.2°F (24.6°C) DP 68.6°F (20.3°C) Grains 105	133.0 (56.1)	53.2 (11.8)	60.2 (132.7)	76,160.0 (22.3)	130.7 (54.8)	52.3 (11.3)	58.2 (128.3)	85,340.6 (25.0)

Notes: DB is the dry-bulb temperature; WB is the wet-bulb temperature; DP is the dew-point temperature; Humidity is given in grains; and LC is the latent capacity.

5.2.1.1 Baseline Configuration[4,5]

In an attempt to verify that the laboratory-installed desiccant system's performance was comparable with the manufacturer-supplied performance data, baseline configuration testing was performed prior to IES testing. The baseline desiccant unit airflow rates were found to be within the range of 76.5 m^3/min to 80.7 m3/min (2,700 to 2,850 scfm) with a face velocity of 262.9 to 277.7 m/min (862.6 to 911.2 ft/min) for the process side and 21.2 to 24.1 m3/min (750 to 850 scfm) for the regeneration side. Process air flow reported by the manufacturer was 68.0 to 70.8 m^3/min (2,400 to 2,500 scfm)—slightly lower than the values observed during the tests. The electrical parasitic loads were measured to be between 5.6 and 5.8 kW.

A comparison of the Integrated Test Facility test data with the manufacturer's test data for the process air circuit is presented in Table 5. There was relatively good agreement between the laboratory baseline configuration and the manufacturer's data for LC. The laboratory results for LC are within +1–5% and +13%, respectively, for the three test conditions.

5.2.1.2 IES Configuration[4,5]

The IES configuration consisted of a MTG with an HRU and DFDD in a series arrangement with respect to the MTG exhaust gas. As previously stated, the microturbine exhaust gas flowed through the HRU, where hot water was produced, then to the regeneration inlet plenum of the DFDD.

The DFDD requires a regenerative air flow of 25.5 m^3/min (900 scfm), and the microturbine's exhaust flow rate of 14.2 m^3/min (500 scfm) was not adequate for this direct-fired desiccant unit. In order to provide the required regenerative air flow, the exhaust gas was mixed with outside air at the same conditions as the process inlet air. During these tests, the temperature of the turbine exhaust gas at the HRU outlet ranged from 122.8 to 136.7°C (253 to 278°F).

Because of ambient air temperatures and the microturbine being located outdoors, the turbine maximum power output was limited to 25 kW during the tests. Tabulated DFDD latent capacity results for two different microturbine outputs (20 kW and 25 kW) and the direct-fired baseline configuration at three different process/outside air inlet conditions are shown in Table 6.

Increasing the power output by 25% from 20 to 25 kW results in an LC increase of 18 to 45%, depending on the process/outside air inlet conditions. The IES maximum LC was observed at the dry-/wet-bulb conditions of 29.4/24.3°C (85.0/75.8°F) and the minimum at 26.7/19.7°C (80.0/67.4°F). The DFDD

unit LC at the maximum and minimum conditions with a microturbine power output of 25 kW is only 58 and 35% of the baseline direct-fired capacity. A microturbine with a minimum exhaust flow rate of at least 25.5 m^3/min (900 scfm) would not require mixing of exhaust gas with outside air and should yield better results from the desiccant dehumidification unit.

To show the improvement in IES efficiency with utilization of the waste heat, the efficiencies of the MTG only, the MTG and HRU, and the total IES (MTG, HRU, and DFDD) at various power levels are shown in Fig. 14. The efficiencies for each configuration were determined by the ratio of the total energy output to the total energy input. For the IES configuration, the total energy output consisted of the electric power output generated by the MTG, the heat recovered by the HRU, and the LC of the desiccant dehumidification unit.

The energy input included the gas input (based on the HHV of the gas) to the MTG and the electrical parasitics (all the power used by the fans, pumps, and electronics of the MTG, desiccant, and HRU units).

Addition of the DFDD to the MTG and HRU configuration resulted in increased overall IES efficiency at all power levels with higher IES efficiencies and efficiency increments at higher kW output. Specifically, the IES efficiency increased by 7% from approximately 53% to 60% with addition of the DFDD (based on the HHV of the natural gas) at 25 kW (85,361 Btu/h) MTG power output.[5]

5.2.2 Indirect-Fired Desiccant Dehumidification System[4]

An IES configuration consisting of the MTG, HRU, and the IFDD was tested at the IES laboratory facility to determine the effects of power output of the MTG on the LC and latent LCOP of the IFDD, as well as on the overall IES efficiency. In this configuration, the regeneration heat source was a hot water loop interfacing with a heating coil in the IFDD. Heat is transferred to the water loop from the MTG exhaust through the HRU.

The maximum water loop flow rate through the HRU was ~5.8 m^3/h (~26 gpm) with a maximum hot water temperature of ~91°C (~196°F). The actual temperature depends on several parameters such as MTG output,

Mode of operation	Process/outside air* inlet conditions °F (°C)			Regeneration inlet plenum** conditions °F (°C)			Latent capacity Btu/h (kW)
	DB[1]	WB[2]	DP[3]	DB[1]	WB[2]	DP[3]	
Direct-Fired	80.0 (26.7)	67.4 (19.7)	61.0 (16.1)	80.0 (26.7)	67.4 (19.7)	61.0 (16.1)	80,815.4 (23.7)
IES 20 kW				131.5 (55.3)	85.6 (29.8)	69.6 (20.9)	24,038.1 (7.0)
IES 25 kW				150.8 (66.0)	90.8 (32.7)	72.0 (22.2)	28.426.7 (8.3)
Direct-Fired	95.0 (35.0)	75.0 (23.9)	66.5 (19.2)	95.0 (35.0)	75.0 (23.9)	66.5 (19.2)	81,198.1 (23.8)
IES 20 kW				144.0 (62.2)	90.0 (32.2)	73.3 (22.9)	27,436.1 (8.0)
IES 25 kW				167.4 (75.2)	96.0 (35.6)	76.5 (24.7)	39,872.3 (11.7)
Direct-Fired	85.0 (29.4)	75.8 (24.3)	72.4 (22.4)	85.0 (29.4)	75.8 (24.3)	72.4 (22.4)	96,646.6 (28.3)
IES 20 kW				149.3 (66.2)	95.1 (35.1)	81.0 (27.2)	41,862.9 (12.3)
IES 25 kW				168.8 (76.0)	99.6 (37.6)	82.9 (28.3)	56,105.9 (16.4)

* Applicable in IES mode of operation; ** Condition after mixing of exhaust gas with outside air. [1]DB is the dry-bulb temperature; [2]WB is the wet-bulb temperature; [3]DP is the dew-point temperature.

Table 6.
Latent capacity test results (IES-based operation) (Ref. 5)

ambient temperature, and HRU water flow rate. The turbine exhaust gas was at a temperature of ~275°C (~527°F) entering the HRU and ~124°C (~255°F) leaving the HRU.

The ratio of the IFDD LC to the total energy input is the LCOP. The total energy input to the IFDD includes the HRU input on the regeneration heating coil side and electrical parasitics, such as the energy use of the desiccant wheel motor, fans, and electronics. The overall IES efficiency is defined as the ratio of the sum of the net electric power output of the MTG and the LC of the IFDD to the total energy input. The net electrical power output of the MTG consists of the total power generated by the MTG minus the auxiliary power consumed by the IES. The total energy input to the IES includes the gas input to the MTG (based on the higher heating value or HHV of natural gas) and the electrical parasitics (all the power used by the fans, pumps, and electronics of the MTG, HRU, and IFDD).

The test results reported were for MTG net power output varying from 10 to 25 kW. The upper limit was again constrained by ambient conditions. Other test parameters included HRU flow rate of ~5.8 m^3/h (~26 gpm), IFDD dry-/wet-bulb temperature at process and regeneration inlet of 35°C/24°C (95°F/75°F), process/regeneration air flow rate of 76.5 m^3/min (2,700 scfm) and IFDD desiccant wheel speed of 58 rph.[6]

The LC and LCOP as a function of the MTG power output is shown in Fig. 15.[6]

The results indicate that the LC of the IFDD increases with an increase in the MTG output. An increase in MTG output from 10 to 25 kW resulted in an increase in the observed LC from ~11.1 kW to ~18.8 kW (~38,000 Btu/h to ~64,000 Btu/h).

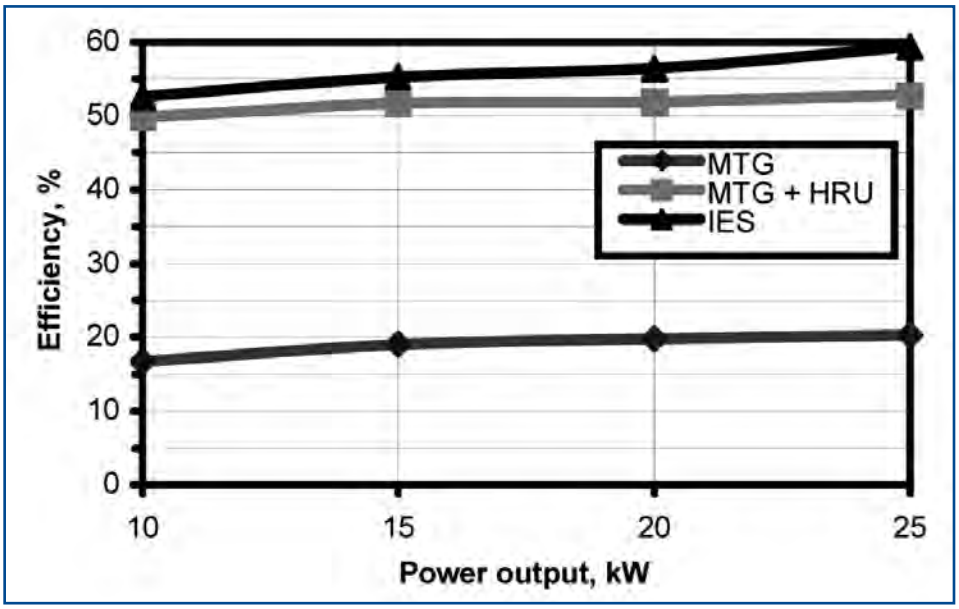

Fig. 14. Efficiencies of microturbine (MTG) and IES. (*Source:* "CHP Integration (OR IES): Maximizing the Efficiency of Distributed Generation with Waste Heat Recovery," Proceedings of the Power Systems 2003 Conference, Clemson, SC, March 2003.)

The LCOP was observed to increase from a minimum of ~46% at a power output of 10 kW to a maximum of ~54% at a power outputs of 15 and 20 kW and decreased to ~51% at a power output of 25 kW. The decrease in LCOP at 25 kW is attributed to the impact of ambient temperature on the operating parameters of the MTG and the heat recovery equipment, as discussed in Sect. 3.4. These test runs were performed at ambient temperatures ranging from 25°C to 30°C (77°F to 86°F).

The effect of the MTG output on the overall IES efficiency is shown in Fig. 16. For comparison, Fig. 16 also shows the effect of the MTG output on the individual unit's efficiency and the combined MTG and HRU efficiency. The combined MTG and HRU efficiency is the efficiency of the IES without the IFDD.[6]

Regarding the efficiencies, the effect of power output is much less pronounced than with the LCOP. After an MTG output of 20 kW, the IES efficiencies start to fall.

Analysis of Fig. 16 shows that the addition of the IFDD to the IES system does not increase its overall efficiency: it drops from 53% (MTG + HRU system) to 34% (MTG + HRU + IFDD system). The drop in efficiency is believed to be due to the parasitic losses in the IFDD.

5.3 ABSORPTION CHILLER[6]

A series of tests were performed on an IES configuration consisting of an MTG, an air-to-water HRU, and a single-effect lithium-bromide/water (LiBr/water) absorption chiller (ABSC). In this arrangement, the MTG's exhaust gas passes through the HRU, generating hot water that is directed to the AC's generator. When the MTG is located outdoors, as in this case,

ambient temperature can be a major factor in the performance when no attempt is made to adjust the inlet air temperature (i.e., air cooling to maintain a constant or lowered inlet air temperature during extremely hot weather).

Higher ambient turbine inlet air temperatures result in lower MTG efficiency, higher exhaust temperatures, higher exhaust heat available for recovery, and higher heat input to the ABSC unit, resulting in better ABSC unit and IES performance. The following sections present the results from tests performed to quantify the effect of ambient air temperature on ABSC unit capacity, COP, and IES efficiency.

An MTG power output setting of 20 kW was selected for this series of tests. This power setting was achievable over the entire wide range of ambient temperatures experienced during the tests, 17.2 to 30°C (63 to 86°F). The hot water flow rate from the HRU and cooling water flow rate from the cooling tower were 0.15 m^3/min (39.8 gpm) and 0.28 m^3/min (74 gpm), respectively. Results will be presented for evaporator chilled water flow rates of 0.07 and 0.13 m^3/min (19 and 34 gpm).

5.3.1 Effect of Ambient Temperature on Absorption Chiller Capacity and COP[6]

The heat input required to drive the ABSC at the full rated load of 35 kW (120,000 Btu/h) of cooling is ~50 kW (172,000 Btu/h). During testing, the maximum heating capacity produced by the MTG + HRU, due to the design features of the HRU and MTG output power setting of 20 kW, was only ~37.9 to 40.8 kW (130,000 to 140,000 Btu/h). Therefore, at a constant MTG power output setting of 20 kW, the ABSC unit could only be driven to ~82% of its full rated load.

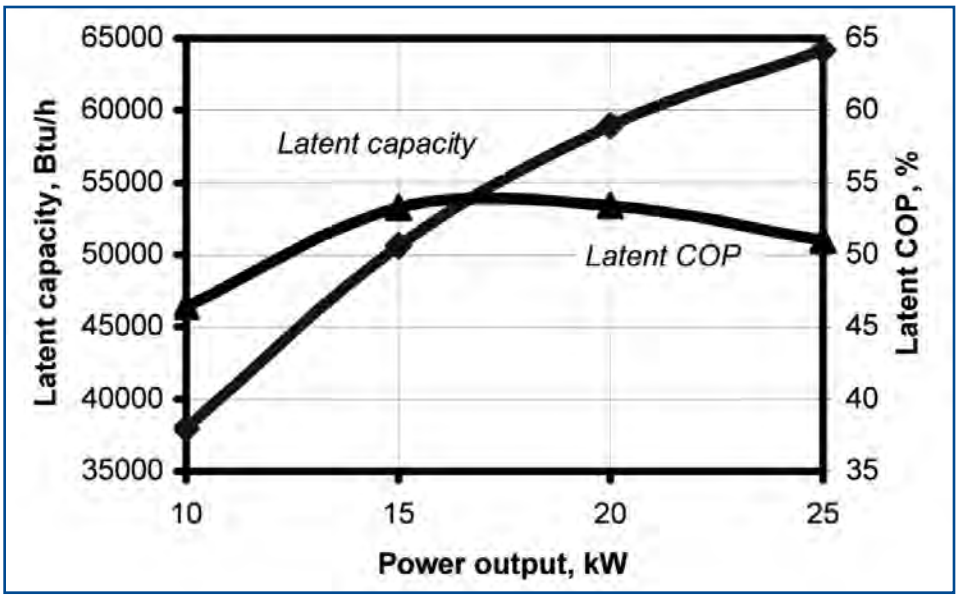

Fig. 15. Effect of power output on latent capacity. (*Source:* "CHP Integration (OR IES): Maximizing the Efficiency of Distributed Generation with Waste Heat Recovery," Proceedings of the Power Systems 2003 Conference, Clemson, SC, March 2003.)

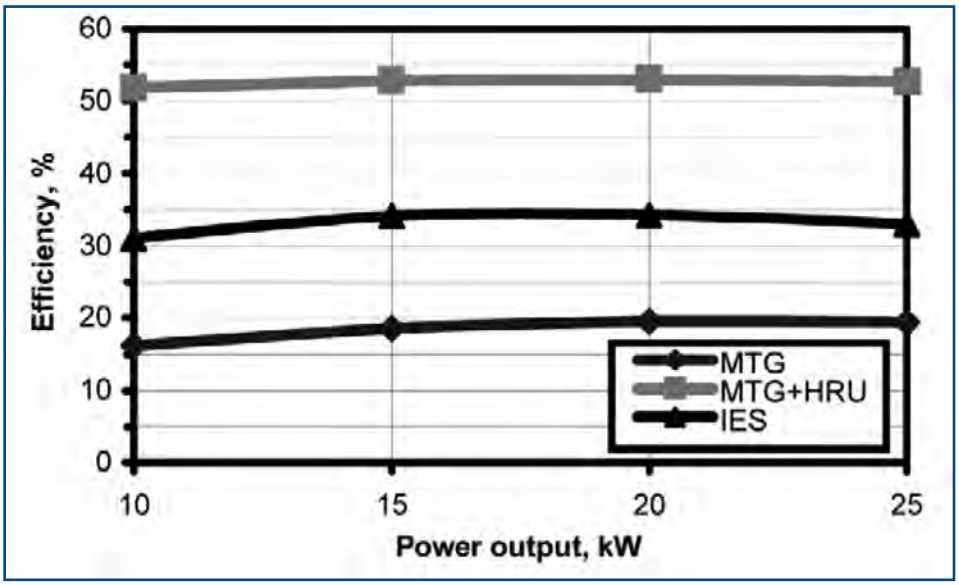

Fig. 16. Effect of power output on efficiency. (*Source:* "CHP Integration (OR IES): Maximizing the Efficiency of Distributed Generation with Waste Heat Recovery," Proceedings of the Power Systems 2003 Conference, Clemson, SC, March 2003.)

The effect of ambient temperature on the ABSC cooling capacity (Q_{chw}) is shown in Fig. 17 for the two chilled-water flow rates (G_{chw}) that were tested.

Based on the increased heat available for input to the ABSC unit with increased ambient temperature, the ABSC unit cooling capacity (Qchw) increase was observed to be nearly linear with ambient temperature from ~19 kW (65,000 Btu/h) at 17.2°C (63°F) to over 26 kW (90,000 Btu/h) at 30°C (86°F) for a Gchw of 19 gpm. At a Gchw of 34 gpm the cooling capacity (Qchw) increase was from ~21 kW (71,000 Btu/h) at 17.2°C (63°F) to ~27 kW (92,000 Btu/h) at 30°C (86°F).

General observations that can be drawn from the test results are that cooling capacity increases with ambient temperature at rates of 1.24% per degree F at a chilled water flow rate of 0.07 m^3/min (19 gpm) and 1.6% per degree F at a chilled water flow rate of 0.13 m^3/min (34 gpm), and cooling capacity increase ranges from 0.77 %/gpm to 2.11%/gpm when the Gchw increases from 19 gpm to 34 gpm.

The COP of the ABSC was defined as the ratio of ABSC cooling capacity, Qchw, to QHRU (AC), the heat supplied by the HRU at the ABSC inlet. Use of the heat supplied at the ABSC inlet takes into account the losses in the hot water loop from the HRU to the AC.

The effect of ambient temperature on the coefficient of performance (COP) of the ABSC is shown in Fig. 18.

The COP increased with ambient temperature from ~57 to ~72% (~0.65% per degree F) at the chilled water flow rate of 0.07 m^3/min (19 gpm) and from ~62 to ~75% (~0.57% per degree F) at the chilled water flow rate of 0.13 m^3/min (34 gpm). Increasing the chilled water flow rate from 0.07 to 0.13 m^3/min (19 to 34 gpm) resulted in COP increases ranging from 2 to 5% (0.133 to 0.33% per gpm). The increased COP with increased chilled water flow rate was calculated without consideration of the increased parasitics required to achieve the higher water flow rate.

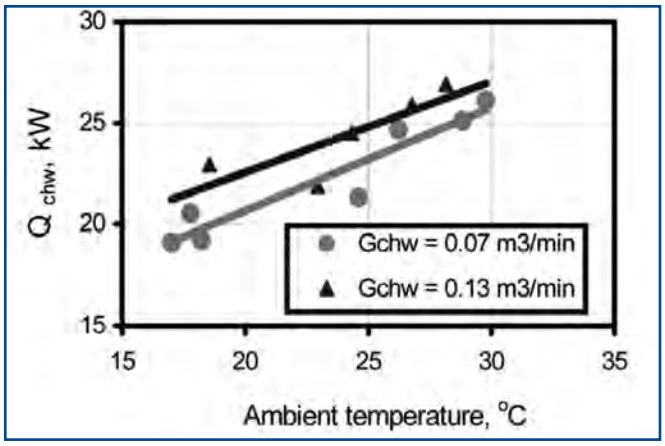

Fig. 17. Effect of ambient temperature on cooling capacity. (*Source*: "Laboratory R&D on Integrated Energy Systems (IES)," Proceedings of the 2003 International Congress of Refrigeration, ICR2003,Washington, DC, August 2003.)

5.3.2 Effect of Ambient Temperature on IES Configuration Efficiency[6]

The effect of ambient temperature on the efficiency of IES MTG + HRU + ABSC configuration is shown in Fig. 19. Also shown in Fig. 19, for comparison, are the efficiencies of various combinations of the MTG, HRU, and ABSC components. The combinations include MTG (producing electric power only), MTG + HRU (producing electric power and heating), and MTG + HRU + ABSC (producing electric power and cooling).

All of the efficiencies, defined as the ratio of the energy output to the energy input, presented in Fig. 19 are based on the HHV of natural gas. When calculating the MTG efficiency, the energy output consisted of the net electric power generated by the MTG, and the energy input was the natural gas input. The energy input and output for the IES configuration of the MTG and HRU were the net electric power generated by the MTG plus the heat recovered by the HRU and natural gas input plus the electric power consumed by the HRU including the booster pump. For the overall IES configuration of the MTG, HRU, and AC, the energy output consisted of the net electric

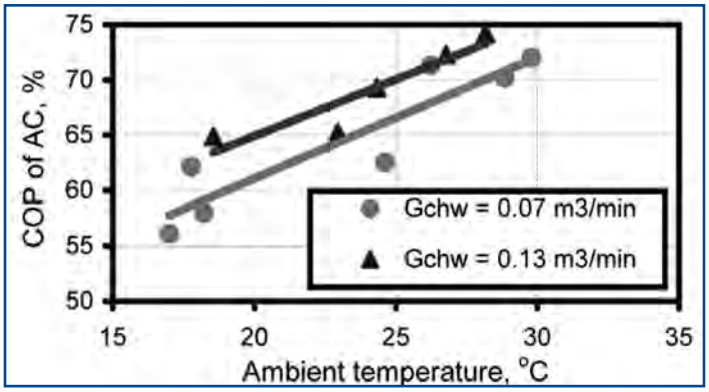

Fig. 18. Effect of ambient temperature on the COP of the absorption chiller. (*Source:* "Laboratory R&D on Integrated Energy Systems (IES)," Proceedings of the 2003 International Congress of Refrigeration, ICR2003,Washington, DC, August 2003.)

power generated by the MTG plus the ABSC cooling capacity, and the energy input consisted of the natural gas input plus the total electric power consumed by the HRU, AC, CT, and pumps.

Tests were performed for chilled water flow rates of 0.07 and 0.13 m^3/min (19 and 34 gpm). The variation in the chilled water flow rate had practically no effect (only a 0.5 to 0.8% average increase) on the overall IES efficiency. Therefore, the efficiency versus ambient temperature for only one flow rate is presented in Fig. 19.

In spite of a decrease in MTG efficiency (20–18%) with ambient temperature, the two IES configuration overall efficiencies increased with ambient temperature. The MTG + HRU configuration showed an efficiency range of 53 to 55% over the ambient temperatures experienced during the test while the MTG + HRU + ABSC configuration yielded an efficiency range of 37 to 42%.

Addition of the ABSC to the MTG + HRU configuration resulted in a decrease in IES efficiency ranging from 16 to 13%, indicating, as expected, that using the waste heat to generate hot water for end use is more efficient than generating hot water for use to drive a single-effect absorption ABSC unit with a nominal COP of 0.7.

5.4 ABSORPTION CHILLER AND DIRECT-FIRED DESICCANT DEHUMIDIFICATION[6]

In the previous IES configuration (MTG + HRU + AC) the temperature of the exhaust gas leaving the HRU and discharging to the environment is in many cases sufficient for use in regenerating the desiccant in a DFDD.

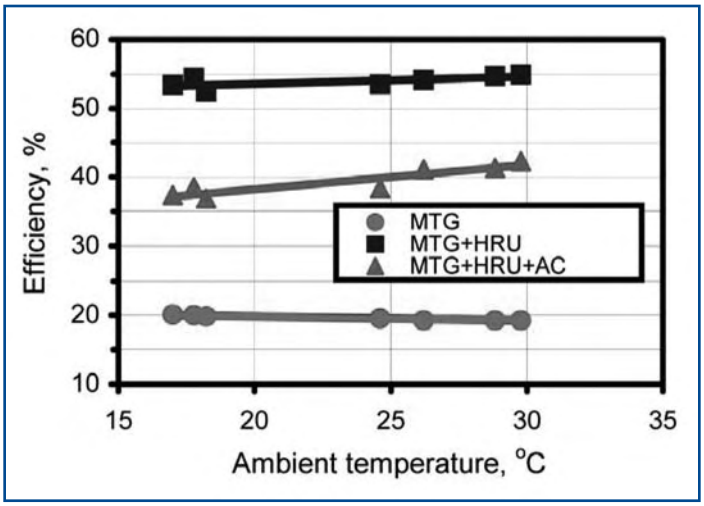

Fig. 19. Effect of ambient temperature on the efficiency of IES configurations. (*Source:* "Laboratory R&D on Integrated Energy Systems (IES)," Proceedings of the 2003 International Congress of Refrigeration, ICR2003, Washington, DC, August 2003.)

Addition of a DFDD to this configuration will increase the utilization of the MTG waste heat and the efficiency of the IES. A series of tests were performed to compare a MTG + HRU + ABSC + DFDD configuration with the previously tested configurations.

The LC and LCOP of the DFDD increase with an increase in process air dew-point or humidity ratio. Therefore, the series of tests were performed at the two DFDD process inlet dry-/wet-bulb temperature conditions of 29.4/24.3°C (85/75.8°F) and 35.0/23.9°C (95/75°F). The corresponding dew-point conditions were 22.4°C (72.4°F) and 19.2°C (66.5°F), respectively. At both inlet process air conditions, MTG power output, hot water, cooling water, and chilled water flow rates were held approximately constant at the measured conditions listed in Table 7.

Also listed in Table 7 are the major performance parameters (i.e., HRU heat capacity, ABSC cooling capacity, and DFDD latent capacity) measured at the two process air conditions. As seen in Table 7, the LC of the DFDD for the 22.4°C dew-point condition was much higher than that for the 19.2°C dew-point inlet air.

The MTG exhaust flow rate, ranging from 11.33 to 4.16 m3/min (400 to 500 scfm), passed through the HRU and entered the regeneration inlet plenum of the DFDD. In the regenerative inlet plenum, in order to achieve a required regenerative stream air flow of 25.5 m^3/min (~900 scfm), the MTG exhaust flow was mixed with outside air. The DFDD's air flow rates, measured during the tests, were found to be within the range of 92.60 to 94.58 m^3/min (3,270 to 3,340 scfm) with a face velocity of 318.4–325.3 m/min (1,044.7–1,067.1 ft/min) for the process side and 25.63–25.77 m^3/min (905–910 scfm) with a face velocity of 88.1–88.6 m/min (289.1–290.7 ft/min) for the regeneration side.

The overall IES efficiency with the addition of the DFDD calculated as the ratio of the energy output and the energy input was determined for the two process-air inlet conditions. The energy output consisted of net electric power generated, the ABSC cooling capacity, and the DFDD latent capacity; the energy input included the natural gas input and the total electric power consumed by the HRU, AC, DFDD, CT, and pumps. The efficiencies of the MTG, MTG + HRU, and MTG +

Table 7. Measured performance parameters of the IES with the desiccant dehumidifier

Dry/wet bulb DFDD temperature, °C (°F)	29.4/24.3 (85/75.8)	35.0/23.9 (95/75)
Ambient temperature, °C (°F)	29.5 (85.1)	30.4 (86.7)
MTG net power, kW (Btu/h)	22.9 (78,457.7)	21.7 (74,456.1)
HRU heat capacity, kW (Btu/h)	40.9 (140,067.2)	41.3 (141,622.2)
AC cooling capacity, kW (Btu/h)	26.6 (91,054.0)	28.1 (96,271.1)
DFDD latent capacity, kW (Btu/h)	10.5 (36,107.4)	7.4 (25,388.1)
AC chilled water flow rate, m^3/min (gpm)	0.105 (27.7)	0.104 (27.6)
HRU hot water flow rate, m^3/min (gpm)	0.144 (38.0)	0.143 (37.9)

HRU + ABSC IES configurations were calculated as described in Sect. 5.3.2.

Figure 20 shows the different IES configuration efficiencies for the two dry-/wet-bulb conditions. The addition of the DFDD to the MTG + HRU + ABSC configuration increases the overall IES efficiency by 5–7%. The IES efficiency with the DFDD decreases with a decrease in dry-/wet-bulb temperatures (dew-point and humidity ratio), with all other parameters constant. The (MTG + HRU + ABSC + DFDD) configuration's overall efficiency is still less than the MT + HRU configuration.

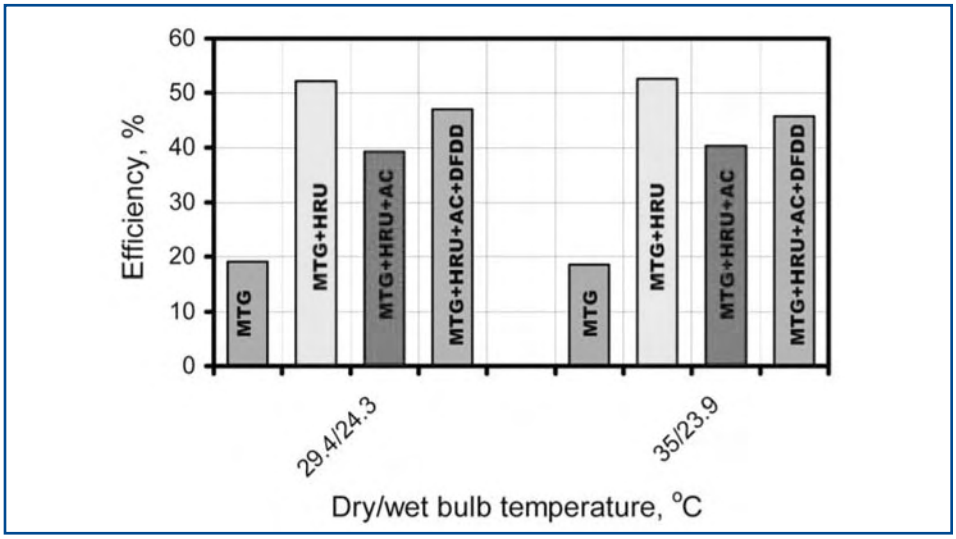

Fig. 20. Efficiencies of IES configurations at various dry-/wet-bulb conditions. (*Source:* "Laboratory R&D on Integrated Energy Systems (IES)," Proceedings of the 2003 International Congress of Refrigeration, ICR2003, Washington, DC, August 2003.)

6. EMISSION TESTS[7]

The objective of the series of emission tests was to study the emissions levels under varying electric loads and microturbine inlet air conditions. The CHP system configuration used for the emissions tests consisted of the 30-kW-rated natural-gas-fired microturbine and the air-to-water HRU. The emissions data was obtained with the microturbine operating over a wide range of power outputs at different ambient temperatures. The basic results are shown in Figs. 21–23 and are discussed in the following sections.

6.1 EFFECT OF MICROTURBINE POWER OUTPUT ON EMISSIONS RATE[7]

During the steady-state emissions tests, microturbine power outputs ranged from one-third to full power (10–28 kW) in 1-kW increments. The full-power output of the microturbine is 30 kW; however, approximately 2 kW is auxiliary power consumed by the microturbine.

Figures 21 and 22 present the CO, NO_x, and SO_2 emissions at the various power outputs in parts per million volume (ppmV) corrected to 15% O2 ($ppmV_{15}$) and converted to mg/m^3. Concentrations of ~36 $ppmV_{15}$ (41 mg/m^3) CO, ~4 $ppmV_{15}$ (8 mg/m^3) NO_x, and ~0.6 $ppmV_{15}$ (1.5 mg/m^3) SO_2 were observed at full power output (28 kW).

As the power output decreases, the concentration of these pollutants changes significantly. The trends of the CO and SO_2 concentrations were similar—both containing two peaks occurring at ~16 kW and 20 kW, while the minimum concentrations were observed to occur at full power output (28 kW). At a power output of ~15 kW, the maximum NO_x concentration

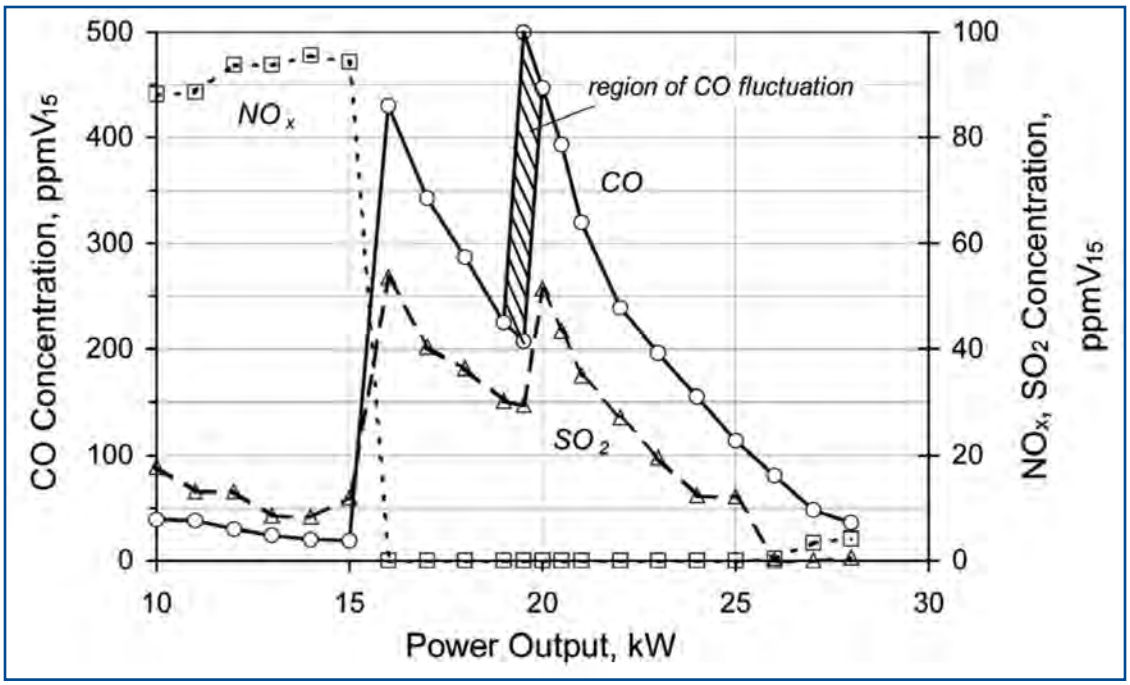

Fig. 21. Concentration of CO, NO_x, and SO_2 ($ppmV_{15}$) vs microturbine power output. (*Source:* "Environmental Aspects of Operation of a Gas-Fired Microturbine-Based CHP System," Proceedings of the 19th Annual International Pittsburgh Coal Conference, Pittsburgh, PA, September 2002.)

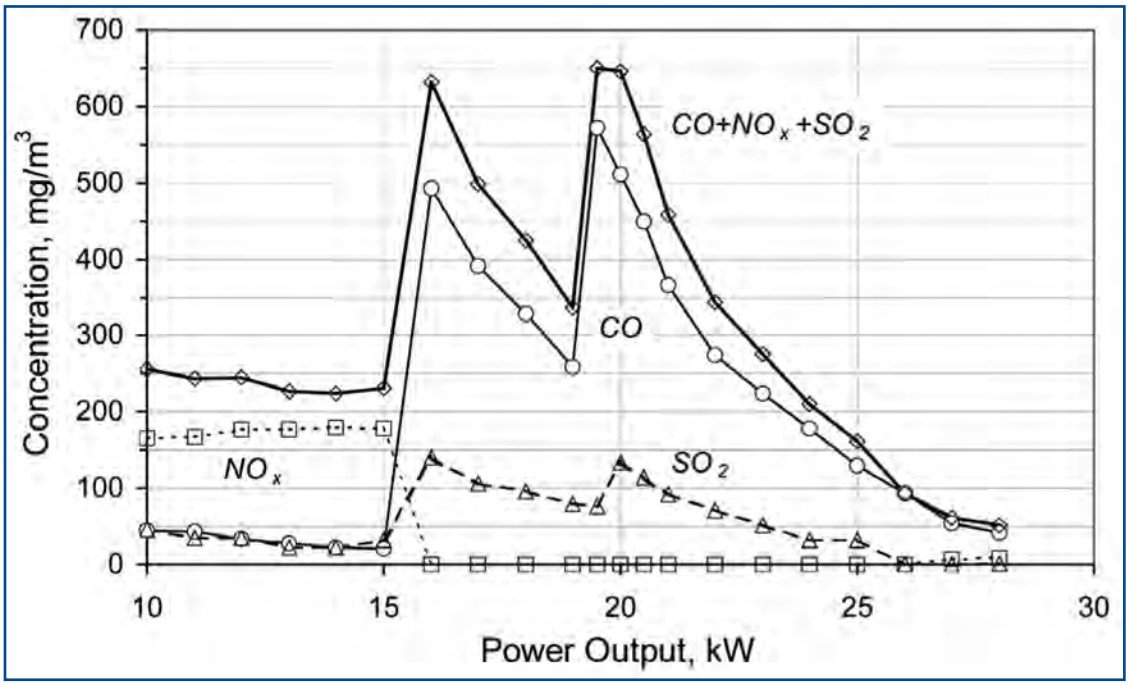

Fig. 22. Concentration of CO, NO_x, and SO_2 (mg/m^3) vs power output. (*Source:* "Environmental Aspects of Operation of a Gas-Fired Microturbine-Based CHP System," Proceedings of the 19th Annual International Pittsburgh Coal Conference, Pittsburgh, PA, September 2002.)

occurred. In order to minimize emissions, a microturbine-based CHPsystem should be sized for and operated as close to full power output as possible.

6.2 EFFECT OF MICROTURBINE INLET AIR ON EMISSIONS RATE[7]

Special tests were performed at MTG power output settings of 25 and 30 kW to study the effect of microturbine air inlet temperature on the emissions rate of the microturbine-based CHP system. In this test, the air inlet temperature and ambient temperature varied throughout the day and from day to day and season to season, depending on weather conditions. The other parameters remained

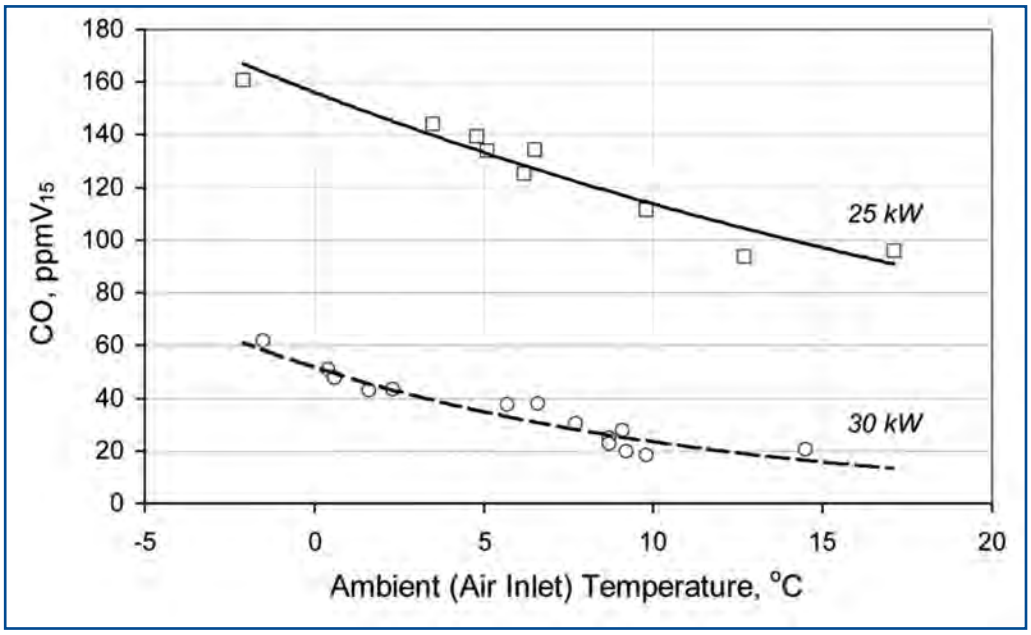

Fig. 23. CO concentration vs air inlet temperature at 25- and 30-kW power output settings. *(Source:* "Environmental Aspects of Operation of a Gas-Fired Microturbine-Based CHP System," Proceedings of the 19th Annual International Pittsburgh Coal Conference, Pittsburgh, PA, September 2002.)

constant during the tests. The only flue gas pollutant significantly affected by a change in microturbine air inlet temperature was CO. As shown in Fig. 23, at both 25- and 30-kW power output, the CO concentration levels decreased with higher air inlet temperatures.

7. THE TECHNOLOGY IN PERSPECTIVE

The major benefits of a DER/CHP are (1) local control of power generation, (2) efficient use of waste heat, (3) increased overall efficiency, and (4) a reduction in emissions.

Local power generation applications include continuous power generation, remote power generation for facilities isolated from the grid, cogeneration, provision of a peaking operation to reduce purchase of electricity during high-price periods, and provision of electrical service at a high level of reliability and quality.

Technologies that can be driven by the DER waste heat in a CHP system include (1) chillers and desiccant dehumidifiers for space cooling and dehumidification, (2) steam generators for space heating, and (3) heat exchangers for process and domestic hot water. These CHP systems can maximize energy efficiency, provide an option for central power generation, and improve electric power reliability and quality.

8. REFERENCES

1. "DER Performance Testing of a Microturbine-Based Combined Cooling, Heating, and Power (CHP) System," Proceedings of Power System 2002 Conference, Clemson, SC, March 2002.
2. "Integration of Distributed Energy Resources and Thermally-Activated Technologies," DistribuTech Conference, Miami Beach, FL, February 2002.
3. "Experimental and Theoretical Study of Gas Micro-turbine-Based BCHP System," Proceedings of the 2001 ASME International Mechanical Engineering Congress and Exposition, AES-23622, New York, NY, November 2001.
4. "CHP Integration (OR IES): Maximizing the Efficiency of Distributed Generation with Waste Heat Recovery," Proceedings of the Power Systems 2003 Conference, Clemson, SC, March 2003.
5. "Baseline and IES Performance of a Direct-Fired Desiccant Dehumidification Unit under Various Environmental Conditions," 2003 ASHRAE Transactions of the Annual Meeting, KC-03-5-2, Kansas City, MI, June 2003.
6. "Laboratory R&D on Integrated Energy Systems (IES)," Proceedings of the 2003 International Congress of Refrigeration, ICR2003, Washington, DC, August 2003.
7. "Environmental Aspects of Operation of a Gas-Fired Microturbine-Based CHP System," Proceedings of the 19th Annual International Pittsburgh Coal Conference, Pittsburgh, PA, September 2002.
8. ASHRAE Handbook, Refrigeration 2002, Chapter 41, "Absorption Cooling, Heating, and Refrigeration Equipment.

Log on to FEMP's Web site for information about New Technology Demonstrations

www.eere.energy.gov/femp/

You will find links to

- A New Technology Demonstration Overview
- Information on technology demonstrations
- Downloadable versions of publications in Adobe Portable Document Format (pdf)
- A list of new technology projects under way
- Electronic access to a regular mailing list for new products when they become available
- How Federal agencies may submit requests to us to assess new and emerging technologies

A Strong Energy Portfolio for a Strong America

Energy efficiency and clean, renewable energy will mean a stronger economy, cleaner environment, and greater energy independence for America. Working with a wide array of state, community, industry, and university partners, the U.S. Department of Energy's Office of Energy Efficiency and Renewable Energy invests in a diverse portfolio of energy technologies.

For More Information

EERE Information Center
1-877-EERE-INF
1-877-337-3464
www.eere.energy.gov/femp

General Contacts

Will Lintner
Team Lead, RSTT
Federal Energy
Management Program
U.S. Department of Energy
1000 Independence Ave, SW
EE-92
Washington, DC 20585
Phone: (202) 586-3120
Fax: (202) 586-3000
william.lintner@ee.doe.gov

Technical Author

Ed Pierce
Oak Ridge National Laboratory
(865) 574-6369
piercefejr@ornl.gov

DOE/EE-0316
May 2007